AD

RESPONSE OF POLYMERS TO TENSILE IMPACT
3. The Integral-Equation, Successive-Substitution Method Applied to Non-Linear Materials having Time-Dependence (Creep, Relaxation)

Approved for public release;
distribution unlimited.

January 1976

**UNITED STATES ARMY
NATICK RESEARCH and DEVELOPMENT COMMAND
NATICK, MASSACHUSETTS 01760**

Food Sciences Laboratory

REPORT DOCUMENTATION PAGE		READ INSTRUCTIONS BEFORE COMPLETING FORM
1. REPORT NUMBER TR-76-36-FSL	2. GOVT ACCESSION NO.	3. RECIPIENT'S CATALOG NUMBER
4. TITLE *(and Subtitle)* RESPONSE OF POLYMERS TO TENSILE IMPACT 3. The Integral-Equation, Successive-Substitution Method Applied to Non-Linear Materials having Time-Dependence (Creep, Relaxation)		5. TYPE OF REPORT & PERIOD COVERED In-House Research
		6. PERFORMING ORG. REPORT NUMBER
7. AUTHOR(s) Prescott D. Crout* Malcolm N. Pilsworth, Jr. Harold J. Hoge		8. CONTRACT OR GRANT NUMBER(s)
9. PERFORMING ORGANIZATION NAME AND ADDRESS US Army Natick Research and Development Command Natick, Massachusetts 01760		10. PROGRAM ELEMENT, PROJECT, TASK AREA & WORK UNIT NUMBERS 1T061102B11A-07
11. CONTROLLING OFFICE NAME AND ADDRESS US Army Natick Research and Development Command Natick, Massachusetts 01760		12. REPORT DATE January 1976
		13. NUMBER OF PAGES 64
14. MONITORING AGENCY NAME & ADDRESS*(if different from Controlling Office)*		15. SECURITY CLASS. *(of this report)* Unclassified
		15a. DECLASSIFICATION/DOWNGRADING SCHEDULE

16. DISTRIBUTION STATEMENT *(of this Report)*

Approved for public release; distribution unlimited.

17. DISTRIBUTION STATEMENT *(of the abstract entered in Block 20, if different from Report)*

18. SUPPLEMENTARY NOTES

* Massachusetts Institute of Technology

19. KEY WORDS *(Continue on reverse side if necessary and identify by block number)*

STRAINS	STRAIN PROPAGATION	NUMERICAL ANALYSIS
STRAIN RATE	POLYMERS	DIGITAL COMPUTERS
PLASTIC DEFORMATION	POLYAMIDE RESINS	STRESS-STRAIN CURVES
TENSILE IMPACT STRENGTH	NONLINEAR ELASTIC MATERIAL	SUCCESSIVE SUBSTITUTION METHOD
	TIME-DEPENDENT MATERIAL	SUCCESSIVE INTEGRATION

20. ABSTRACT *(Continue on reverse side if necessary and identify by block number)*

A better understanding is required of tensile-impact strains in military components such as body armor and parachute straps. A solution for the propagation of strain waves in elastic materials was extended to materials exhibiting creep and relaxation. The basic integral-equation, successive-substitution solution developed in two previous reports was extended using a model with two springs in series and a dashpot in parallel with one of them.

DD _{1 JAN 73} FORM 1473   EDITION OF 1 NOV 65 IS OBSOLETE

20. ABSTRACT (Cont'd)

With appropriate values, the model conformed adequately to experimental tensile-impact data on a 50 cm length of Nylon yarn. For this short specimen, wave reflections confused the experimental data and there was a lack of uniqueness in the computed results. Different choices of model parameters represented the data equally well. Hence impact experiments were made on 400 cm specimens of Nylon yarn in which reflections would not be observed. We were unable to represent these experiments with the model. The experimental data showed that the Nylon contracted after the initial strain pulse had elongated it. 4% strains fell to 3% during a single experiment. Contraction of the material had not been expected and deserves further investigation. Methods of choosing the parameters of the model are presented in an appendix.

Preface

This is the third and last in a series of reports on
high-speed tensile-impact work performed in the Pioneering
Research Laboratory of the US Army Natick Laboratories
(now the US Army Natick Research and Development Command).
The first (NLABS Tech. Rept. 69-18-PR) appeared in
July 1968 and the second (NLABS Tech. Rept. 74-26-PR)
appeared in February 1974.

The first report dealt with the basic mathematical
techniques and their application to a linear material.
The second report extended the method to non-linear
materials that do not exhibit creep or other time de-
pendence. The present report deals with non-linear
materials that do exhibit time dependence. Since all actual
materials exhibit creep and relaxation, it is in the present
report that we can expect to get the best test of the
agreement between the theory and the actual behavior of
materials.

Body armor must be resistant to high-speed impact in
order to stop projectiles and shell fragments. Parachute
straps are subjected to sudden tensile stresses when the
parachute opens and the falling load is suddenly decelerated.
The work described in the present series of reports re-
presents progress toward an understanding of tensile impact
but leaves much still to be done.

1

Contents

3

List of Figures

List of Tables

5

Glossary of Terms

A_{i_j} = first time-integral of the repetitive process, corresponding to the lattice point in the ith column and the jth row.

B_{i_j} = second time-integral of the repetitive process.

C_{i_j} = auxiliary quantity found in the repetitive process.

c = velocity of propagation of strain waves.

c_o = propagation velocity at zero strain.

$f(x)$ = function giving the initial displacement of each particle in a string.

$g(x)$ = function giving the initial velocity of each particle in a string.

i = subscript indicating the column number of a lattice point.

j = subscript indicating the row number of a lattice point.

K = spring constant in the model of the material.

k = a repetition index (superscript) in the repetitive process.

L = length of unstretched sample.

n = number of lattice-point intervals in the length L.

R = $(c/c_o)^2$, a given function of the strain ϵ.

s = displacement of a particle of material from its unstretched position x, also see $\bar{s}$; also, in the appendix, a quantity appearing in Laplace transforms.

$\bar{s}$ = s/Lv_o; the bar is dropped after the quantity is introduced.

s_1 = portion of the displacement s due to spring 1.

6

s_2 = portion of the displacement s due to spring 2.

s_{ij} = displacement of the particle of material at the lattice-point ij from its unstretched position x_{ij}.

$_2s_{ij}$ = portion of s_{ij} due to spring 2.

t = time, also see $\bar{t}$.

$\bar{t}$ = tc/L; the bar is dropped after the quantity is introduced.

v = velocity of a particle of sample.

v_0 = velocity of impacted end of sample.

x = distance of a particle of material from the fixed (left) end of the sample in the un-stretched state, also see $\bar{x}$.

$\bar{x}$ = x/L; the bar is dropped after the quantity is introduced.

α = (appendix) quantity defined by eq (10a); also, a quantity defined by eq (37a).

ϵ = normal strain along axis of string, $= \partial s/\partial x$.

ϵ_1 = portion of ϵ due to spring 1.

ϵ_2 = portion of ϵ due to spring 2.

λ = ratio of length of spring 2 to length of spring 1.

μ = damping constant of the dashpot across spring 2.

$\bar{\mu}$ = μ/c_0L, the normalized value of μ.

ρ = density of unstretched material.

σ = normal stress across spring 1 (total stress along axis of string).

σ_1 = contribution of the dashpot to σ.

σ_2 = contribution of spring 2 to σ.

7

$$\sigma' = (\partial/\partial \chi)\, \sigma(\epsilon_1).$$

τ = time constant of the spring 2-dashpot combination.

ω = (appendix) angular frequency of a small sinusoidal motion imparted to a prestretched string.

8

RESPONSE OF POLYMERS TO TENSILE IMPACT 3. The
Integral-Equation, Successive-Substitution Method
Applied to Non-Linear Materials having Time-
Dependence (Creep, Relaxation)

1. Introduction

The present report is the third of a series of three
that describe the results of mathematical and experimental
investigations of the response of polymers to tensile
impact. Professor Crout is responsible for the mathe-
matical developments, Mr. Pilsworth is responsible for
the experimental data, and all three authors have worked
on the physics of the problem and the writing of the reports.
For further background material reference   1   should be
consulted; it is the first of the present series and is
referred to as Report I. Similarly reference   2   is the
second report of the series and is referred to as
Report II; the present report is of course Report III.

The work was undertaken primarily because of our in-
terest in the production of improved body armor. Ex-
perimental data had been obtained showing the propagation
of strain pulses in nylon string after tensile impact at
moderately high speeds. A theory and mathematical tech-
niques were recognized as important means of explaining what
was observed and of predicting what might occur under other
conditions.

1. P. D. Crout, M. N. Pilsworth, Jr., and H. J. Hoge,
"Response of Polymers to Tensile Impact. 1. An integral-
equation, successive-substitution solution for use in digital
computers, and its application to a linear elastic model",
U.S. Army Natick Laboratories, Technical Report 69-18-PR
(July 1968), 71 p; AD-682714.

2. P. D. Crout, M. N. Pilsworth, Jr., and H. J. Hoge,
"Response of Polymers to Tensile Impact. 2. Extension of
the integral-equation, successive-substitution solution to
non-linear, time-independent materials", U.S. Army Natick
Laboratories, Technical Report 74-26-PR (Feb 1974),
76 p; AD-780811.

In Report I the mathematical method was developed and was applied to the problem of strain propagation in a linear material having no creep or other time dependence. Since the solution of this problem is known, and since the new method gives the correct solution, its validity for this case has been established, and by inference the new method can also be expected to give correct answers to related problems for which satisfactory solutions have not been available.

In Report II the iterative method of Report I was extended to non-linear materials and was applied to a set of experimental data that had been previously analyzed by the method of characteristics. Good agreement was found between the present (iterative) method and the method of characteristics at low and intermediate strains but trouble was encountered at higher strains when the stress-strain curve was concave upward.

In the present report the problem of a non-linear, time-dependent material is treated and compared with experiment. Reports I and II were considered as setting the stage for Report III, for whereas the problems treated in I and II could be solved by other methods, there is no fully satisfactory method of computing the behavior of non-linear, time-dependent materials. The results being presented in the present report do not clear up this situation but represent some progress toward solving it. The methods now being presented are somewhat limited by the tendency toward oscillatory and diverging solutions. This tendency is reduced, as we expected, in the presence of time dependency. In the present report, the greatest weakness of the solutions is some lack of uniqueness: there is too much latitude in the choice of model parameters. A greater range of experimental data would undoubtedly help to resolve this situation.

The experimental data with which we compare our results has mostly been obtained on specimens 50 cm long, in which one and sometimes two reflections of the strain pulse occur during the period of observation. The present report contains comparisons of computed behavior with data in which reflections occur, and it also contains experimental data taken on long specimens in which no reflections occurred during the period of observation. The no-reflection results were surprising and may constitute a major contribution of the present report.

10

2. Summary of Reports I and II

In Report I a new method of handling the problem of strain-wave propagation was developed, in which the relevant partial differential equations are transformed into integral equations. The integral equations are then solved by the method of successive substitutions. Referring to the system shown in Fig. 1, the differential equation

$$\frac{\partial^2 s}{\partial t^2} = c^2 \frac{\partial^2 s}{\partial x^2} \qquad (1)$$

was derived for strain propagation. Here x is the position of a particle of material in the unstrained state, s is the displacement of the same particle from its original position, and c is the wave velocity. For ready reference, these and other definitions are included in a glossary at the beginning of this report. By integrating eq (1) twice, the equation

$$s = f(x) + t\,g(x) + c^2 \int_0^t \int_0^t \frac{\partial^2 s}{\partial x^2} \, dt \, dt \qquad (2)$$

was obtained; this equation is valid when c is constant (a linear material has c constant). The function f(x) specifies the initial displacements and g(x) specifies the initial velocities; except at the impacted end of the string these functions are usually zero in practical problems.

Equation (2) was simplified by putting f and g=o and introducing three new normalized variables:

$$\bar{s} = \frac{s}{L\,v_o}, \quad \bar{t} = \frac{c\,t}{L}, \quad \bar{x} = \frac{x}{L}, \qquad (3)$$

in which v_o is the velocity of the impacted end of the string. The result of these substitutions (see Report I, p 36) was to reduce eq (2) to the form

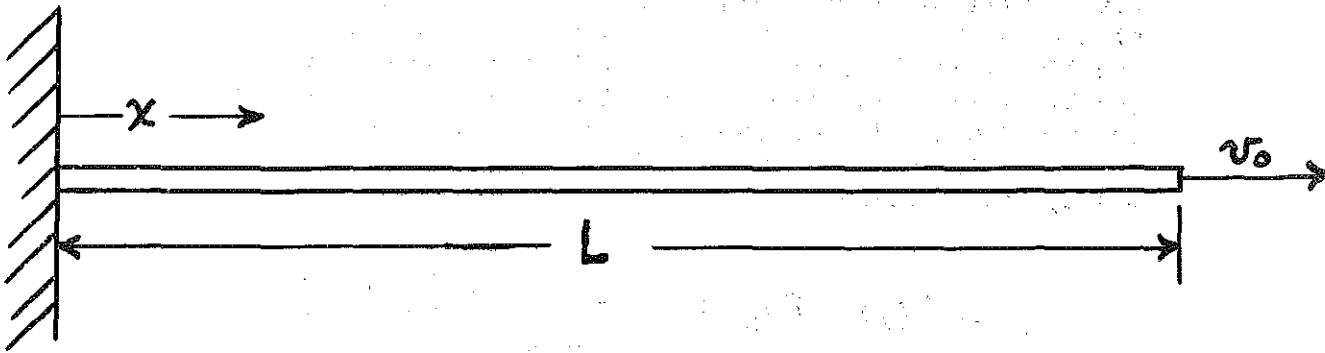$$s = \int_0^t \int_0^t \frac{\partial^2 s}{\partial x^2} \, dt \, dt \qquad (4)$$

11

Fig. 1. String subjected to tensile impact.

where for convenience the bars have been dropped from the new variables. The velocity $\dot{\theta}$ does not appear in eq (4); this equation refers, in fact, to the problem in which L=1, c=1, and $\bar{v}_o$=1. When a solution of eq (4) has been obtained, the results can be applied to actual problems by using eq (3). The method devised for evaluating the integral in eq (4) was to accept a lattice of points in the (x,t) plane, to specify the values of s along three borders of this lattice, and to find the values of s at the remaining points by an iterative procedure. To find values of the integrand the three-point differentiation formula was used, and for the integration the trapezoidal formula was adopted. Values of s were calculated one row (one value of t) at a time by iteration, using the border values, and taking all other starting values from the previous row. When the specified degree of convergence had been reached, the next row of values was calculated.

Two linear, time-independent problems were solved in Report I. In the first the end of the string is set in motion with its full velocity v_o at t=o; in the second the velocity rises linearly during a finite time-interval beginning at t=o. The solutions found by iteration were compared with the exact solutions, which are known. The agreement was good except where the exact solution had a discontinuity (abrupt rise, wave front). In the neighborhood of a discontinuity the values (of strain, for example) calculated by iteration oscillated above and below the exact values, when plotted versus x. It was clear that the iterative process could not give results that reproduced a discontinuity exactly. This had been anticipated. In adjusting to a discontinuity the iterative results were found to be first too low, then too high, and so on, but as the discontinuity traveled away from any particular point, the amplitude of the oscillations near that point was found to decrease.

The second of the problems solved in Report I, in which the rise in velocity occurred during a finite time interval, was more easily handled by the iterative procedure than the problem in which the velocity rise was instantaneous. This was of course expected. There was still some oscillation of the iterative values above and below the exact solution but not enough to destroy the usefulness of the solution. The conclusion reached in Report I was that the successive substitution procedure was satisfactory and that oscillations relative to the exact solution could be troublesome but would probably not be serious. The greatest chance of trouble was expected to be associated with calculations based on a stress-strain curve that was concave upward; in such cases shock waves are mathematically predicted, for example by the method of characteristics.

13

In Report II it was shown that a non-linear, time-independent material may be handled in a manner similar to a linear material, but with eq (4) replaced by

$$\bar{A}(\bar{X},\bar{t}) = \int_0^{\bar{t}} \int_0^{\bar{t}} \left(\frac{c}{c_o}\right)^2 \frac{\partial^2 \bar{A}}{\partial \bar{X}^2} \, d\bar{t} \, d\bar{t} \, . \qquad (5)$$

This equation differs from eq (4) only in the presence of the factor $(c/c_0)^2$. The other variables in the two equations are the same, although in Report II and eq (5) the bars over the variables have not been dropped. The propagation velocity c is a function of ϵ, and c/c_0 is the ratio of the velocity at strain ϵ to the velocity at strain zero. An accepted stress-strain curve permits c/c_0 to be found. For use in the repetitive process the quantity $R \equiv (c/c_0)^2$ was expressed in a form convenient for machine calculation, usually as a polynomial in ϵ. The function $R(\epsilon)$ was not changed during any one computational run.

As a test of the usefulness of the successive-substitution method for non-linear, time-independent systems, a problem was selected that had been previously solved by the method of characteristics. The values of R were obtained from the same stress-strain curve that had been used in the method-of-characteristics solution. Good agreement was obtained between the successive-substitution solution and the method-of-characteristics solution, from the time of impact up until the time when the method-of-characteristics predicted that shock waves were beginning to develop and the successive-substitution method began to give serious oscillations. The two sets of results are compared in Fig. 2; the lines show strain as a function of position, calculated by successive substitutions; the plotted points are corresponding strains calculated by the method of characteristics. All the points and the corresponding curves show good agreement except for two points near the top of the figure. These points and the corresponding curve were in the region of developing shock waves and increasing oscillations.
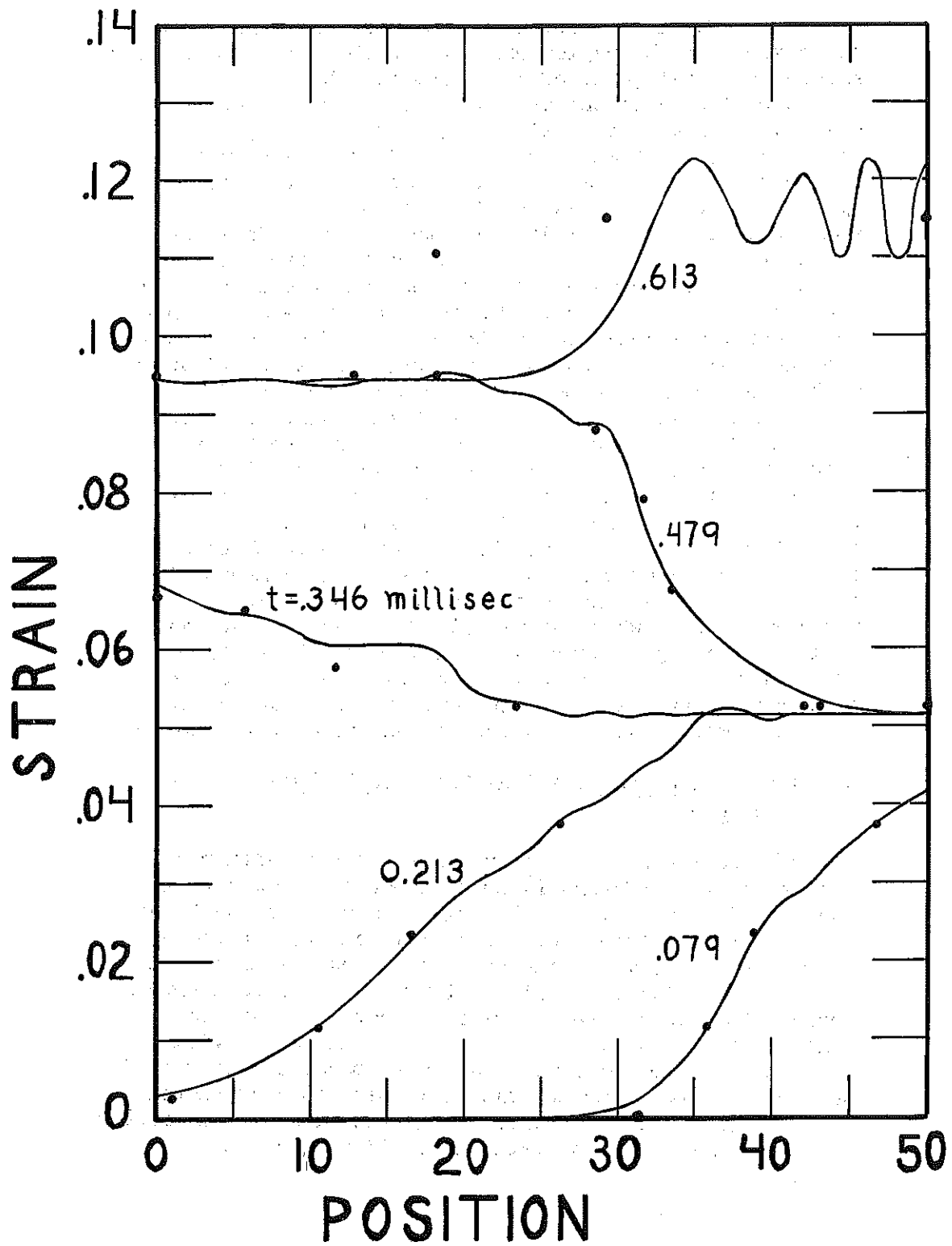
Fig. 2. Strain pattern for nylon yarn calculated by
successive substitution (lines), and by method-
of-characteristics (points).

The successive-substitution solution could not be made to converge in the region where the method of characteristics showed the development of shock waves. This as we know is the region where the stress-strain curve is concave upward. In order to obtain a solution of sorts, the accepted stress-strain curve was modified slightly by replacing the final part of the concave-upward section by a straight line; this avoided divergence of the solution. It was concluded that the solution does not immediately diverge in a region where the stress-strain curve is concave upward but diverges when the computed wave front becomes very steep. The question arose as to whether the shock waves indicated by the method of characteristics and the oscillations shown by the successive-substitution method were simply computational results not found in actual materials. This was a tempting assumption, since we know of no cases where a tensile shock wave has ever actually been observed. However, it was concluded that the possibility of actual oscillations in strain along the length of a string could not be ruled out. A considerable portion of Report II was devoted to showing that such oscillations can in fact serve as a means of conserving energy. In this connection it should be remembered that, when the method of characteristics is applied in a region where a shock wave develops, the solution satisfies momentum and continuity but does not conserve energy. In using it, one has to assume an unspecified mechanism to convert the excess energy into heat.

3. Extension of the Previous Solution to Include Time-Dependence

The results obtained previously apply to either a linear material (Report I) or to a non-linear material (Report II) but they do not apply to a material that shows time-dependence (creep or stress relaxation). Since most materials show time-dependence the methods of Reports I and II are of limited applicability, unless experiments are devised that take place so rapidly that creep and relaxation are insignificant. In extending the previous solution to problems involving time-dependence, we wished to choose a model for our material that could adequately describe the time-dependence and at the same time introduce no more additional mathematical complications than necessary.

16

Choice of Model System

The model adopted is shown in Fig. 3. It consists of a spring and dashpot in parallel, with a second spring in series with the combination. This model was discussed briefly in Report I. It has been widely used. Smith[3], for example, uses it in a problem involving nylon yarn. His treatment differs from ours, however, because his springs are linear (stress = a constant x strain) whereas our springs are in general non-linear. Both Smith's dashpot and ours are linear; that is, the force supported by the dashpot is proportional to the rate of change of strain.

A three-element model was accepted as probably the simplest that could show the desired time dependence. The two-element models both have drawbacks. A spring and dashpot in parallel (Voigt model) obeys the differential equation:

$$\sigma = a \epsilon + b \frac{d\epsilon}{dt}. \qquad (6)$$

This model allows creep but cannot represent stress relaxation at constant strain. A spring and dashpot in series (Maxwell model) obeys the equation

$$\frac{d\epsilon}{dt} = c\sigma + d\frac{d\sigma}{dt}. \qquad (7)$$

This model gives an incorrect creep behavior because the creep continues indefinitely at a constant rate, whereas the materials of interest to us show a decreasing creep rate. The accepted model (Fig. 3) avoids the two drawbacks just mentioned, but of course its validity has to be established by experiment. As will appear later, the model has been found adequate in the sense that by adjusting the various parameters our experimental data could usually be well represented. It is of course possible that some other model would have been equally satisfactory. It is even possible that a simple Voigt or Maxwell model would have been adequate for some of our data, considering that we were dealing with high-speed impact and rather short intervals of time, but the adequacy of these simple models was not anticipated.

3. J. C. Smith, "Wave Propagation in a Three-Element Linear Spring and Dashpot Model Filament", J. Appl. Phys. 37, 1697-704 (15 Mar 1966).
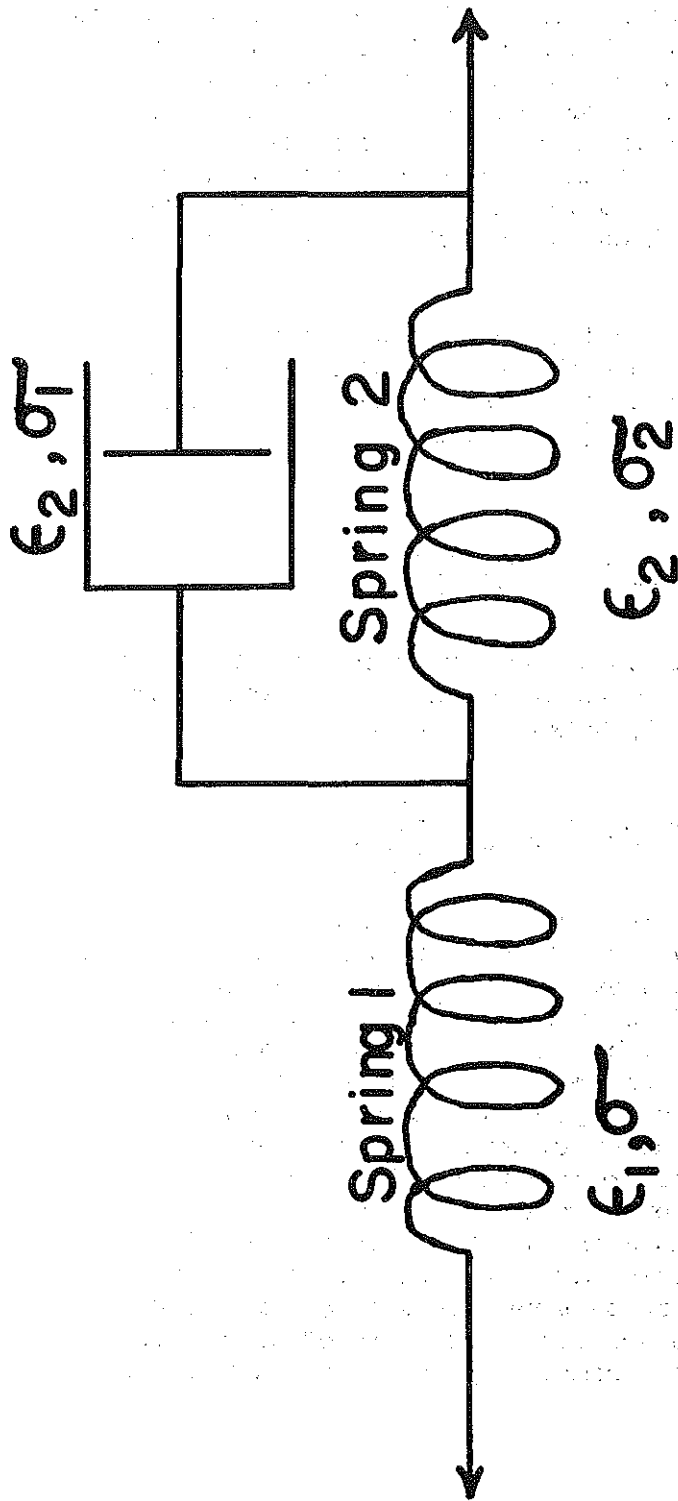
Fig. 3. Model adopted for use in this report.

18

The analysis of the model shown in Fig. 3 was carried out in such a way that the two springs could obey different stress-strain curves, but when the time came for actual calculations the assumption was made that the two springs were alike except in "length". The length of spring 2 was taken to be λ times the length of spring 1. If the same stress could be applied to both springs, the strains would obey the relation

$$\epsilon_2 = \lambda \epsilon_1 . \tag{8}$$

Of course the stresses across the two springs are in general unequal, because the dashpot across spring 2 supports part of the stress. The ratio of spring lengths, λ, was one of the parameters to be adjusted in order to fit the experimental data.

As a second disposable parameter the damping constant μ of the dashpot was used. In the simple case where spring 2 is linear with spring-constant K the constant μ is simply related to the time constant of the system consisting of spring 2 and the dashpot across it; we have

$$\mu = K \tau \tag{9}$$

where τ is the time constant.

In addition to assigning the values of λ and μ we also have some freedom in the choice of the stress-strain curve used for both springs.

Mathematical Analysis of the Time-Dependent Model. The model of a time-dependent material shown in Fig. 3 can be analyzed by making certain additions and changes in the methods used in Reports I and II. The separate spring 1 is equivalent to the "springs" handled in Report II. The spring 2, with the dashpot across it, forms a new combination that has not been previously treated.

More specifically we shall suppose that a cubic centimeter of the material behaves like the mechanical system shown in Fig. 3. Because of the unit length and cross-section the strains may be considered to be elongations, and the stresses to be forces. The basic equations are

$$\sigma = \sigma_1 + \sigma_2 \tag{10}$$

$$\epsilon = \epsilon_1 + \epsilon_2 \qquad (11)$$

$$\sigma = \sigma(\epsilon_1) \qquad (12)$$

$$\sigma_2 = \sigma_2(\epsilon_2) \qquad (13)$$

$$\sigma_1 = \mu \frac{d\epsilon_2}{dt}. \qquad (14)$$

We thus consider the elongation ϵ to be composed of two parts, one of which depends on the total stress alone, whereas the other depends also on the time (past history). Similarly, we consider the force σ to be composed of two parts, one of which depends on ϵ_2 alone, whereas the other is proportional to $d\epsilon_2/dt$. The springs shown in Fig. 3 are in general not linear. In the above equations the effect of inertia is not included.

In the case of our string the above relations pertain to each point, and (14) becomes

$$\sigma_1 = \mu \frac{\partial \epsilon_2}{\partial t}; \qquad (15)$$

also, we regard the displacement s to be composed of two component displacements, thus

$$s = s_1 + s_2 \qquad (16)$$

where, in accordance with (11)

$$\frac{\partial s}{\partial x} = \epsilon, \qquad (17)$$

$$\frac{\partial s_1}{\partial x} = \epsilon_1, \qquad (18)$$

$$\frac{\partial s_2}{\partial x} = \epsilon_2. \qquad (19)$$

20

Finally, the condition for dynamic equilibrium is expressed by

$$\rho \frac{\partial^2 \Delta}{\partial t^2} = \frac{\partial \sigma}{\partial \chi} \qquad (20)$$

(See Report II, eq 6).

We shall consider the damping coefficient μ to be constant, which corresponds to viscous damping.

Integrating (15) we obtain

$$\epsilon_2 = (\epsilon_2)_{t=0} + \frac{1}{\mu} \int_0^t \sigma_1 \, dt \; ; \qquad (21)$$

also, integrating (20) twice gives

$$\Delta = (\Delta)_{t=0} + t \left(\frac{\partial \Delta}{\partial t}\right)_{t=0} + \frac{1}{\rho} \int_0^t \int_0^t \frac{\partial \sigma}{\partial \chi} \, dt \, dt . \qquad (22)$$

The problem in which we are interested is one in which the initial distributions of displacement, velocity, and strain are zero. In this case (21) and (22) become, respectively,

$$\epsilon_2 = \frac{1}{\mu} \int_0^t \sigma_1 \, dt \; ; \qquad (23)$$

$$\Delta = \frac{1}{\rho} \int_0^t \int_0^t \frac{\partial \sigma}{\partial \chi} \, dt \, dt . \qquad (24)$$

In view of (12) and (18), (24) may be written

$$\Delta = \frac{1}{\rho} \int_0^t \int_0^t \sigma'(\epsilon_1) \frac{\partial^2 \Delta_1}{\partial \chi^2} \, dt \, dt . \qquad (25)$$

Proceeding as in Report II, page 7, we now place

$$\bar{\Delta} = \frac{\Delta}{L} \; , \quad \bar{\chi} = \frac{\chi}{L} \; ; \quad \bar{t} = \frac{c_0 t}{L} \qquad (26)$$

where

$$c = \sqrt{\frac{\sigma'(\epsilon_1)}{\rho}} \; , \quad c_0 = \sqrt{\frac{\sigma'(0)}{\rho}} \, . \qquad (27)$$

c and c_0 hence pertain to the left hand spring in Fig. 3. It now follows that

$$\epsilon_1 = \frac{\partial \Delta_1}{\partial x} = \frac{L}{L} \frac{\partial \bar{\Delta}_1}{\partial \bar{x}} = \frac{\partial \bar{\Delta}_1}{\partial \bar{x}} = \bar{\epsilon}_1 \, . \qquad (28)$$

Similarly

$$\epsilon_2 = \bar{\epsilon}_2 \, , \quad \text{and} \quad \epsilon = \bar{\epsilon} \, . \qquad (29)$$

From (27) and (28) we see that

$$c(\epsilon_1) = c(\bar{\epsilon}_1) = c\left(\frac{\partial \bar{\Delta}_1}{\partial \bar{x}}\right) . \qquad (30)$$

(23) now becomes

$$\bar{\epsilon}_2 = \frac{L}{c_0 \mu} \int_0^{\bar{t}} \sigma_1 \, d\bar{t}$$

or, placing

$$\bar{\mu} = \frac{c_0 \mu}{L} \, , \qquad (31)$$

we have

$$\bar{\epsilon}_2 = \frac{1}{\bar{\mu}} \int_0^{\bar{t}} \sigma_1 \, d\bar{t} \, . \qquad (32)$$

22

(25) becomes

$$\bar{s}\, L = \frac{L^2}{\rho\, c_0^2 L} \int_0^{\bar{t}} \int_0^{\bar{t}} \sigma'(\bar{\epsilon}_1) \frac{\partial^2 \bar{s}_1}{\partial \bar{x}^2}\, d\bar{t}\, d\bar{t},$$

or, noting (27),

$$\bar{s} = \int_0^{\bar{t}} \int_0^{\bar{t}} R(\bar{\epsilon}_1) \frac{\partial^2 \bar{s}_1}{\partial \bar{x}^2}\, d\bar{t}\, d\bar{t} \qquad (33)$$

where

$$R(\bar{\epsilon}_1) = \left(\frac{c(\bar{\epsilon}_1)}{c(0)}\right)^2 = \left(\frac{c}{c_0}\right)^2. \qquad (34)$$

A possible method of successive substitutions is now given by the following equations, which are used in the order given, and in which the bars are omitted, it being understood that the various quantities are normalized as indicated on the preceding pages. The step numbers (k) or $(k+1)$ are indicated by superscripts. Starting with $\epsilon_1^{(k)}$ and $\epsilon_2^{(k)}$ we obtain $\epsilon_1^{(k+1)}$ and $\epsilon_2^{(k+1)}$ by the following steps:

$$\epsilon_2^{(k+1)} = \frac{1}{\mu} \int_0^{t} \left[\sigma(\epsilon_1^{(k)}) - \sigma_2(\epsilon_2^{(k)})\right] dt, \qquad (35)$$

$$s^{(k+1)} = \int_0^{t} \int_0^{t} R(\epsilon_1^{(k)}) \frac{\partial \epsilon_1^{(k)}}{\partial x}\, dt\, dt, \qquad (36)$$

$$\epsilon_1^{(k+1)} = \frac{\partial s^{(k+1)}}{\partial x} - \epsilon_2^{(k+1)}. \qquad (37)$$

23

We note that in this successive substitution process it is not required that a record be kept of s_1, s_2, s or ϵ . The initial and boundary conditions are

$$s(0,t) = 0 \qquad 0 \leq t ,$$

$$s(x,0) = 0 \qquad 0 \leq x \leq 1,$$

$$s(1,t) = \text{given function of } t. \qquad (38)$$

Since these conditions are on s, it does not appear that we shall be able to confine our attention to the strains alone. Accordingly, we shall place (36) in the form

$$s^{(k+1)} = \int_0^t \int_0^t R(\epsilon_1^{(k)}) \frac{\partial^2 s_1^{(k)}}{\partial x^2} \, dt \, dt. \qquad (39)$$

Since s_1 and s_2 are both positive, it follows from (38) that

$$s_1(0,t) = 0 \quad \text{and} \quad s_2(0,t) = 0 \quad \text{when} \quad 0 \leq t$$

$$s_1(x,0) = 0 \quad \text{and} \quad s_2(x,0) = 0 \quad \text{when} \quad 0 \leq x \leq 1. \qquad (40)$$

From the second of these equations we also have

$$\epsilon_1(x,0) = 0 \quad \text{and} \quad \epsilon_2(x,0) = 0 \quad \text{if} \quad 0 \leq x \leq 1; \qquad (41)$$

also, since

$$\epsilon_2(1,t) = \frac{1}{\mu} \int_0^t \sigma_1(1,t) \, dt , \qquad (42)$$

24

and since σ_1 is finite, we see that $\epsilon_2(l,t)$ cannot be changed abruptly from its initial value of zero regardless of what motion is specified for the right end of the string. On the other hand $\epsilon_1(l,t)$ may change abruptly. Similarly, since

$$\epsilon_2(x,t) = \frac{1}{\mu} \int_0^t \sigma_1(x,t)\, dt \qquad (43)$$

we see that <u>for any fixed value of x, $\epsilon_2(x,t)$ is a continuous function of t.</u>

We shall now consider a tentative numerical procedure for applying the above equations. As before, we shall use a square lattice, as indicated in Fig. 4. The various quantities are determined one row at a time; hence, we need only describe how to obtain data for the jth row when data for the preceding rows are available. The various steps are as follows.

1) s is known exactly at i=o and i=n for all values of j. As a first approximation we shall take the values of s for the (j-1)th row as those for the jth row when $0 < i < n$. Similarly, we shall take the values of s_2 for the (j-1)th row as the first approximation to those of the jth row. Subtracting $s_2^{(1)}$ from $s^{(1)}$ we obtain $s_1^{(1)}$ for the jth row.

2) Knowing $s_1^{(1)}$ for the jth row we determine $\epsilon_1^{(1)}$ for this row; and hence, using (39), $s^{(2)}$ for this row.

3) Knowing $\epsilon_1^{(1)}$ for the jth row, $\epsilon_2^{(2)}$ is determined for this row using (35). This is a subroutine process of successive substitution.

4) Integrating $\epsilon_2^{(2)}$ numerically, $s_2^{(2)}$ for the jth row is obtained.

5) $s_1^{(2)}$ for the jth row is obtained by subtracting $s_2^{(2)}$ from $s^{(2)}$. We note that s is known exactly at the end points.

6) We now proceed as with step 2, and so on.

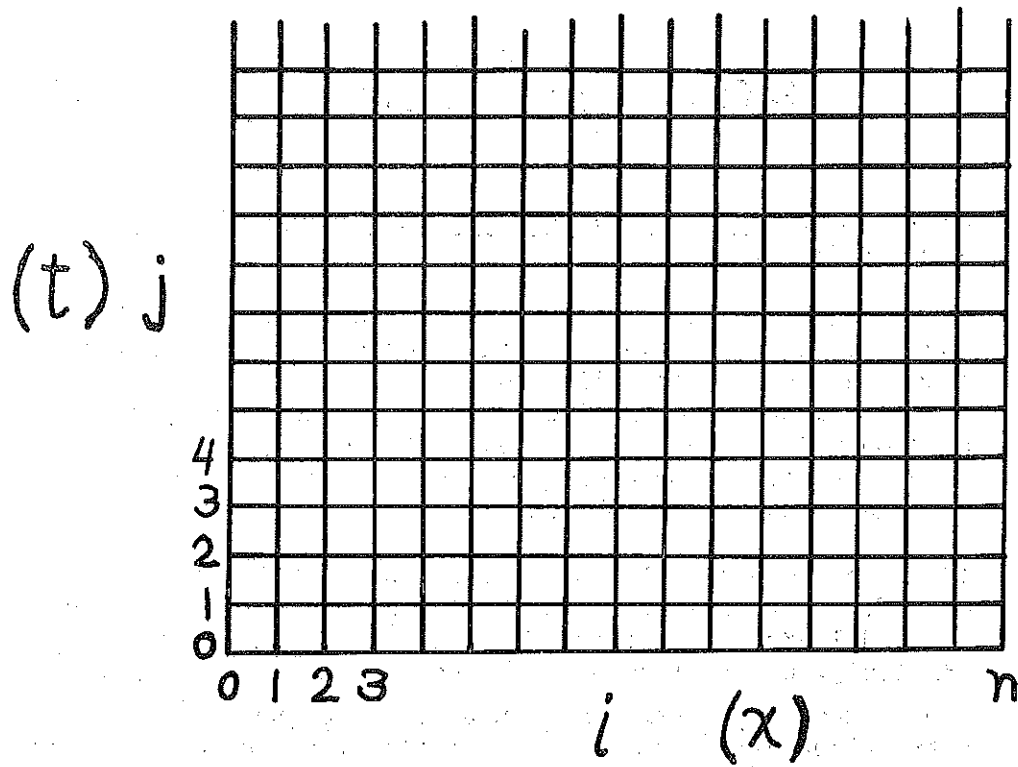Fig. 4.   Lattice of points at which calculations
are to be made.

26

In the various numerical differentiations and integrations
appropriate formulas are used. To fix ideas we can
tentatively say that the numerical integrations will be
carried out using the trapezoidal formula (116 Report I);
and that second derivatives will be obtained using the
three point formula (117 Report I), based on a
quadratic polynomial. Except at end points first de-
rivatives will be obtained using the three point formula

$$f'(x) = \frac{1}{2h}\left[f(x+h) - f(x-h)\right] \qquad (44)$$

based on a quadratic polynomial; at the end points they
will be obtained using the two point formula

$$f'(x) = \frac{1}{h}\left[\pm f(x) \mp f(x \mp h)\right] \qquad (45)$$

based on the linear polynomial, the upper sign being
used at the right end, and the lower sign being used at
the left.

Proceeding along the lines indicated above, the set
of instructions given in the next section for programming
the successive repetition process for use in connection
with a digital computer was devised. In these in-
structions A is a measure of the first time integral in
(39), B is a measure of the second; and C is a measure of
the time integral in (35). Instead of finishing the
calculation of ϵ_2 for each round of the main successive
repetition process, which is aimed at solving (39), the
subroutine indicated in 3) above is replaced by a single
round of the subroutine process. This was done because
it was felt that there was no point in calculating ϵ_2 to
an accuracy much greater than ϵ_1 during the course of
the main successive repetition process. However, if
difficulty is encountered with convergence, it may be
necessary to include the full subroutine process. Mean-
while, until such difficulty is encountered we shall use
the simpler process described in the instructions.

In the above discussion $s^{(k)}$ and $s_2^{(k)}$ are the basic quantities which we know at the beginning of the kth round; and $s^{(k+1)}$ and $s_2^{(k+1)}$ are the quantities which we ultimately calculate during the course of the round. If, however, we use $s^{(k)}$ and $\epsilon_2^{(k)}$ as the basic quantities, we avoid the situation wherein ϵ_2 is integrated to give s_2, which is then differentiated to give ϵ_2. The result is the set of instructions given in the next section.

4. <u>Description of the Repetitive Process when Applied to the Nonlinear String with Creep or Relaxation</u>

Our problem is to determine the values of the quantities s_{ij} and $_2s_{ij}$ at the points of a square lattice. i takes the values 0, 1, 2, 3, $\cdots$,n; and j takes the values 0, 1, 2, 3, $\cdots$. n is given; hence the range of values taken by i is bounded. The range of values taken by j, however, has no upper bound except, possibly, one which will be assigned later from practical considerations, Fig. 4.

The values of s_{ij} are given for those points which lie on the border, thus

$$\left. \begin{aligned} s_{0j} &= 0 & j &= 0, 1, 2, 3, \cdots; \\ s_{i0} &= 0 & i &= 1, 2, 3, \cdots n; \\ s_{nj} &\text{ is given}, & j &= 0, 1, 2, 3, \cdots. \end{aligned} \right\} \quad (46)$$

The values of $_2s_{ij}$ are given for those points which lie on the left and lower parts of the border, thus

$$\left. \begin{aligned} _2s_{0j} &= 0, & j &= 0, 1, 2, 3, \cdots; \\ _2s_{i0} &= 0, & i &= 0, 1, 2, 3, \cdots n. \end{aligned} \right\} \quad (47)$$

The values of s_{ij} and $_{2}s_{ij}$ at the other points are determined a row at a time— that is, for j fixed and i = 1, 2, 3, ··· , (n - 1) for s_{ij}, and n for $_{2}s_{ij}$. The values of j are taken in the order 1, 2, 3, ···. In view of this it will evidently be sufficient to describe how to obtain the values of s_{ij} and $_{2}s_{ij}$ for the jth row when the values for all of the preceding rows are known.

The values of s_{ij} and $2^{s_{ij}}$ for the jth row are obtained as the limits gotten, respectively, by applying repeatedly a process shortly to be described. At the beginning of the kth repetition we have the quantities

$$s_{1j}^{(k)}, \; s_{2j}^{(k)}, \; s_{3j}^{(k)}, \cdots , \; s_{m-1,j}^{(k)},$$
$$_{2}s_{1j}^{(k)}, \; _{2}s_{2j}^{(k)}, \; _{2}s_{3j}^{(k)}, \cdots , \; _{2}s_{mj}^{(k)}, \tag{48}$$

as approximations to the quantities

$$s_{1j}, \; s_{2j}, \; s_{3j}, \cdots , \; s_{m-1,j},$$
$$_{2}s_{1j}, \; _{2}s_{2j}, \; _{2}s_{3j}, \cdots , \; _{2}s_{mj}, \tag{49}$$

respectively. <u>Here k is a superscript, not an exponent.</u> When the process is applied starting with the quantities (48), the quantities

$$s_{1j}^{(k+1)}, \; s_{2j}^{(k+1)}, \; s_{3j}^{(k+1)}, \cdots \; s_{m-1,j}^{(k+1)},$$
$$_{2}s_{1j}^{(k+1)}, \; _{2}s_{2j}^{(k+1)}, \; _{2}s_{3j}^{(k+1)}, \cdots , \; _{2}s_{mj}^{(k+1)}, \tag{50}$$

are obtained as approximations to (49), respectively. The sequence of repetitions is started by taking the values of s_{ij} and $2^{s_{ij}}$ for the $(j-1)^{th}$ row as approximations to the values for the jth row, respectively, thus

$$s_{1j}^{(1)} = s_{1,j-1}, \; s_{2j}^{(1)} = s_{2,j-1}, \cdots , \; s_{m-1,j}^{(1)} = s_{m-1,j-1},$$
$$_{2}s_{1j}^{(1)} = _{2}s_{1,j-1}, \; _{2}s_{2j}^{(1)} = _{2}s_{2,j-1}, \cdots , \; _{2}s_{mj}^{(1)} = _{2}s_{m,j-1}. \tag{51}$$

These values are, of course, known. The sequence of repetitions is terminated when for sufficiently large k, the output (50) duplicates the input (48) to the required accuracy. The common values which then compose (48) and (50) are then taken as the final result (49). The values of s_{ij} and 2^s_{ij} which compose the jth row are thus determined.

Finally we shall describe the process by which we start with (48) and obtain (50). During the course of the calculations we compute and record, in addition to the quantities s_{ij} and 2^s_{ij}, the auxiliary quantities $_1\epsilon_{ij}$, $_2\epsilon_{ij}$, R_{ij}, σ_{ij}, $_2\sigma_{ij}$, A_{ij}, B_{ij} and C_{ij}. Along the lower border, where j=o these quantities are defined to be

$$_1\epsilon_{00} = 0, \quad _1\epsilon_{10} = 0, \quad _1\epsilon_{20} = 0, \cdots, \quad _1\epsilon_{m0} = 0;$$

$$_2\epsilon_{00} = 0, \quad _2\epsilon_{10} = 0, \quad _2\epsilon_{20} = 0, \cdots, \quad _2\epsilon_{m0} = 0;$$

$$R_{10} = 1, \quad R_{20} = 1, \quad R_{30} = 1, \cdots, R_{m-1,0} = 1;$$

$$\sigma_{00} = \sigma(0) = 0, \quad \sigma_{10} = \sigma(0) = 0,$$
$$\sigma_{20} = \sigma(0) = 0, \cdots, \sigma_{m0} = \sigma(0) = 0; \tag{52}$$

$$_2\sigma_{00} = \sigma_2(0) = 0, \quad _2\sigma_{10} = \sigma_2(0) = 0,$$
$$_2\sigma_{20} = \sigma_2(0) = 0, \cdots, _2\sigma_{m0} = \sigma_2(0) = 0;$$

$$A_{10} = 0, \quad A_{20} = 0, \quad A_{30} = 0, \cdots, A_{m-1,0} = 0;$$

$$B_{10} = 0, \quad B_{20} = 0, \quad B_{30} = 0, \cdots, B_{m-1,0} = 0;$$

$$C_{00} = 0, \quad C_{10} = 0, \quad C_{20} = 0, \cdots, C_{m0} = 0.$$

The quantities R_{ij}, A_{ij}, and B_{ij} do not exist at the points of the left border, where i=o, or the points of the right border, where i=n. As is the case with s_{ij} and 2^s_{ij} the auxiliary quantities $_1\epsilon_{ij}$, $_2\epsilon_{ij}$, R_{ij}, σ_{ij}, $_2\sigma_{ij}$, A_{ij}, B_{ij}, and C_{ij} are obtained one row at a time, are known in the first (j-1) rows, and are obtained in the jth row as the limits approached by the quantities $_1\epsilon_{ij}^{(k)}$, $_2\epsilon_{ij}^{(k)}$, $R_{ij}^{(k)}$, $\sigma_{ij}^{(k)}$, $_2\sigma_{ij}^{(k)}$, $A_{ij}^{(k)}$, $B_{ij}^{(k)}$, and $C_{ij}^{(k)}$, respectively, during the course of the successive repetitions. The desired basic process is now described by the relations

$$_2\Delta_{ij}^{(k)} = \frac{1}{n}\left(\frac{1}{2}\,_2\epsilon_{0j}^{(k)} + _2\epsilon_{1j}^{(k)} + _2\epsilon_{2j}^{(k)} + \cdots \right.$$
$$\left. + _2\epsilon_{i-1,j}^{(k)} + \frac{1}{2}\,_2\epsilon_{ij}^{(k)}\right) \tag{53}$$
$$i = 1, 2, 3, \cdots, n;$$

$$_1\epsilon_{ij}^{(k)} = \frac{n}{2}\left(s_{i+1,j}^{(k)} - s_{i-1,j}^{(k)} - _2\Delta_{i+1,j}^{(k)} + _2\Delta_{i-1,j}^{(k)}\right) \tag{54}$$
$$i = 1, 2, 3, \cdots, n-1;$$

$$_1\epsilon_{0j}^{(k)} = n\left(s_{1j}^{(k)} - _2\Delta_{1j}^{(k)}\right); \tag{55}$$

$$_1\epsilon_{nj}^{(k)} = n\left(s_{nj}^{(k)} - s_{n-1,j}^{(k)} - _2\Delta_{nj}^{(k)} + _2\Delta_{n-1,j}^{(k)}\right); \tag{56}$$

$$R_{ij}^{(k)} = R\left(_1\epsilon_{ij}^{(k)}\right), \quad i = 1, 2, \cdots, n-1; \tag{57}$$

$$A_{ij}^{(k)} = A_{i,j-1} + R_{i,j-1}\left[\frac{1}{2}\left(s_{i-1,j-1} + s_{i+1,j-1}\right.\right.$$
$$\left. - _2\Delta_{i-1,j-1} - _2\Delta_{i+1,j-1}\right) - s_{i,j-1} + _2\Delta_{i,j-1}\right] \tag{58}$$
$$+ R_{ij}^{(k)}\left[\frac{1}{2}\left(s_{i-1,j}^{(k)} + s_{i+1,j}^{(k)} - _2\Delta_{i-1,j}^{(k)}\right.\right.$$
$$\left. - _2\Delta_{i+1,j}^{(k)}\right) - s_{ij}^{(k)} + _2\Delta_{ij}^{(k)}\right],$$
$$i = 1, 2, \cdots, n-1;$$

31

$$B_{ij}^{(k)} = B_{i,j-1} + \tfrac{1}{2}\left(A_{i,j-1} + A_{ij}^{(k)}\right),$$
$$i = 1, 2, \cdots, m-1; \qquad (59)$$

$$A_{ij}^{(k+1)} = 0.3\, A_{ij}^{(k)} + 0.7\, B_{ij}^{(k)}, \quad i = 1,2,\cdots,m-1; \qquad (60)$$

$$\sigma_{ij}^{(k)} = \sigma\left(_1\epsilon_{ij}^{(k)}\right), \quad i = 0,1,2,\cdots,m; \qquad (61)$$

$$_2\sigma_{ij}^{(k)} = \sigma_2\left(_2\epsilon_{ij}^{(k)}\right), \quad i = 0,1,2,\cdots,m; \qquad (62)$$

$$C_{ij}^{(k)} = C_{i,j-1} + \tfrac{1}{2}\left(\sigma_{i,j-1} - {}_2\sigma_{i,j-1} + \sigma_{ij}^{(k)} - {}_2\sigma_{ij}^{(k)}\right)$$
$$i = 0,1,2,\cdots,m; \qquad (63)$$

$$_2\epsilon_{ij}^{(k+1)} = 0.3\,{}_2\epsilon_{ij}^{(k)} + 0.7\,\frac{1}{\mu m}\, C_{ij}^{(k)}. \qquad (64)$$

5. Application of the Method to Experimental Data (with Reflections)

In order to test the model selected for a time-dependent material and to test the successive-substitution method developed in the preceding mathematical analyses, a set of experimental data obtained on a nylon yarn was selected. This set of data was originally presented and analyzed by Pilsworth and Hoge[4]. It was used in Report II as the basis for a comparison between the results of a successive-substitution analysis and the best of the method-of-characteristics analyses given in Ref. 4. All of the data were obtained from the high-speed stroboscopic photograph shown in Fig. 3 of reference 4, which is

4. M. N. Pilsworth, Jr., and H. J. Hoge, "Rate-Dependent Response of Polymers to Tensile Impact", Textile Res. J. 35, 129-39 (Feb 1965).
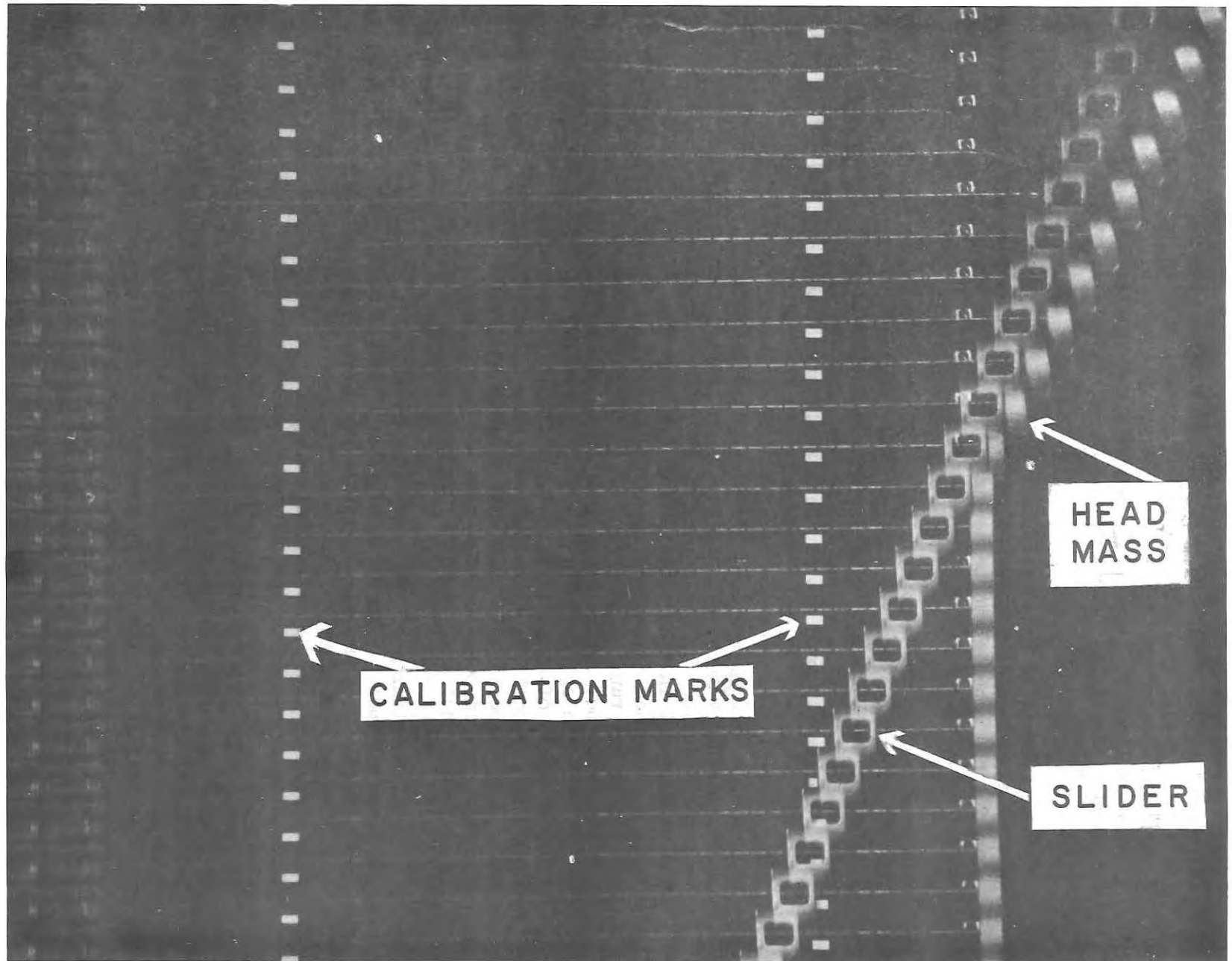
Fig. 5. Photo of nylon during tensile impact. The data obtained from this photo were selected for use in the present paper. The speed of impact was 90 m sec^{-1} and the successive exposures were made at the rate of 7500 sec^{-1}.

reproduced as Fig. 5 of the present report. This figure
contains 6 usable exposures following impact, and the
strains obtained from these exposures are plotted as
the broken lines of Figs. 7, 8, and 9, where they are
compared with results from three different computer
runs.

Each attempt to calculate the behavior of the nylon
yarn as experimentally observed requires a stress-strain
curve for the material to be accepted; it also requires
values to be chosen for the parameters λ and μ .
We began by using the stress-strain curve that had
previously given the best results. This is curve C in
Fig. 6; it is also curve C in Fig. 5 of reference 4.
This curve had been developed by successive trials in
which the method of characteristics was used and it
gave a reasonably good fit of the experimental data,
especially the early data obtained before the second or
third reflection of the strain pulse had occurred. The
values of λ and μ required for a calculation were
chosen partly by guesswork and partly by methods similar
to those described in the appendix, but more primitive.
The values used in each computer run are given in
Table 1, together with other relevant quantities
describing the run. After each run had been plotted
and analyzed, new values of λ , μ or other relevant
quantities were selected for use in the next run.
Since no table of computer runs was included either in
Report I or Report II, a complete table is included in
the present report. All runs that yielded useful in-
formation are listed. Omitted runs had faulty programs,
diverged very quickly, or had other defects.

Results of three of the best runs are shown in
the present report. The first of these, Run 14, is
shown in Fig. 7, where strain is plotted against position,
with time as a parameter. The 6 solid lines are plotted
from 6 rows of the computer print-out, one row being
chosen to correspond to each of the 6 usable exposures
in Fig. 5. The common time of each exposure and the
corresponding row of the print-out is indicated near
each pair of curves in the figure. Good agreement
between calculation and experiment is indicated if each
pair of curves nearly coincides. In Fig. 7 the agree-
ment is only fair. One of the weaknesses of earlier
calculations has been taken care of. Figure 2 shows
regions of constant strain near x = 0 for two curves
(t = 0.479 and 0.613); it also shows such regions
near x = 50 for three curves (t = 0.213, 0.346,
and 0.479). The experimental data do not show these
flat regions. Run 14 does not have the flat regions
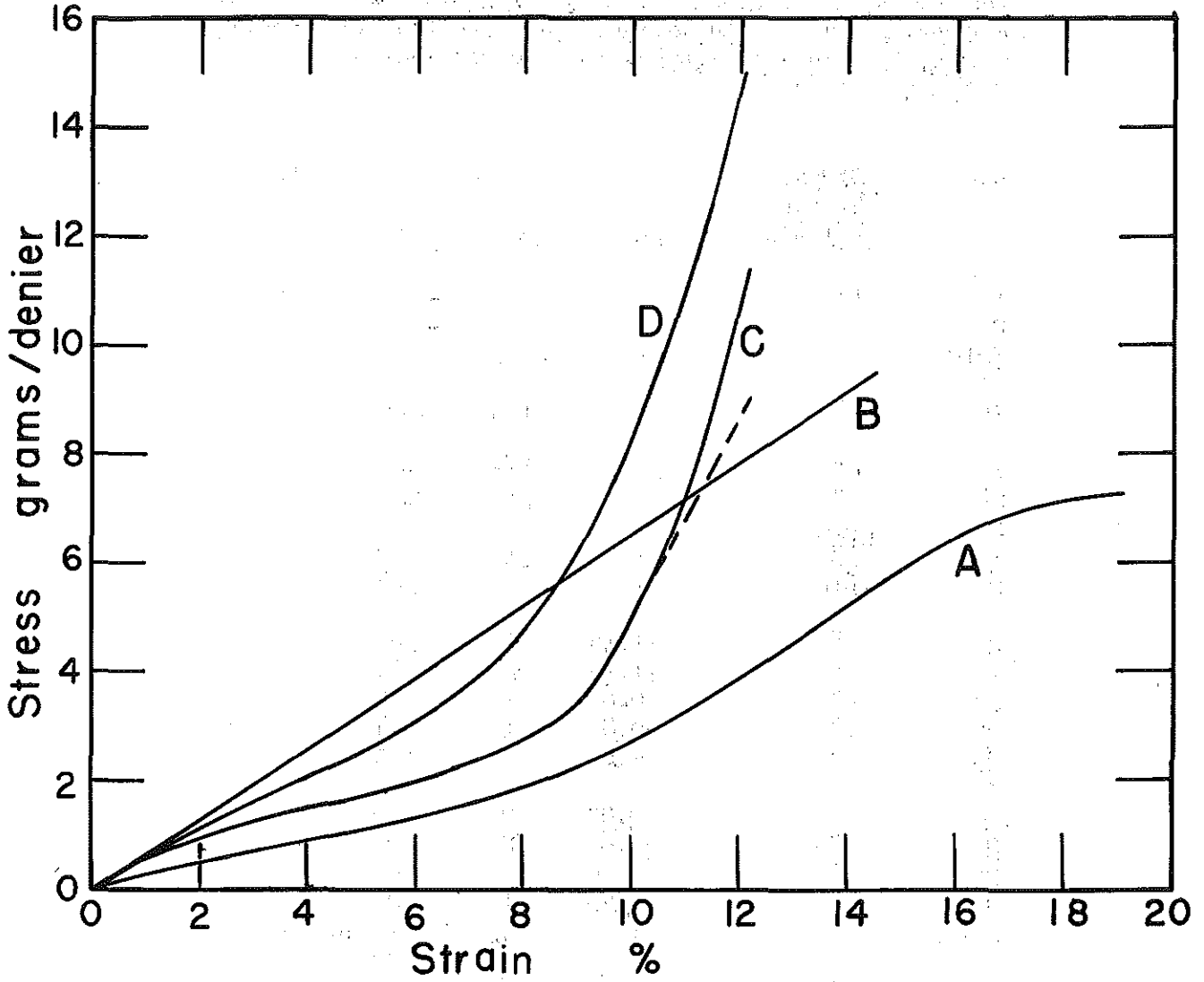and in this respect represents an advance over the

Fig. 6. Various stress-strain curves for nylon; A,
semi-static; B, linear; C and D, dynamic but
developed with different assumptions.

Table 1. Summary of Computer Runs

All significant computer runs are listed, including those made for the present report and also those made for Reports I and II. The omitted runs had faulty programs, diverged at an early stage, or were considered not useful for other reasons.

Run	Stress-Strain Relation	R	λ	μ	Notes
1	Lin	-	-	-	a
2	"	-	-	-	
3-10	C	-	-	-	b
11	"	-	-	-	c
12	"	-	1/3	240	d
13	"	-	1/3	60	
14	"	-	1	60	
15	Lin	1	1	60	g
16	D	-	1	60	g
20	Lin	1	1	24	
21	"	1.15	1	24	g
22	"	1.15	2	60	
23	"	0.85	1	60	
24	"	0.85	1	24	
25	"	0.85	2	120	
26	"	0.85	2	60	
27	Lin	0.85	2	24	
28	"	.70	1	60	
29	"	.70	1	24	
30-33	"	1	1 or 3	7.5 or 30	e
35	"	25/16	1/9	61.218	
36-41	C	-	1 to 25	3.9 to 30	
42	A	-	5	11.25	
43-49	Lin (2)				f

36

Notes for Table 1

a Runs 1-2, treated in Report 1.

b Runs 3-11, treated in Report 2.

c Curve C unmodified (no linear final section).

d Runs 12-29, treated in the present report; they
   refer to short specimens with strain reflections.

e Runs 30-33, 36-42, treated in the present report,
   runs without reflections.

f Runs 43-49, treated in Appendix 2 of Report 2;
   stress-strain curve consisted of 2 linear sections
   of slopes 1:4.

g Runs 15, 16, 21 gave best agreement with the ex-
   perimental data of all runs made, with 21 probably
   the best of the 3.
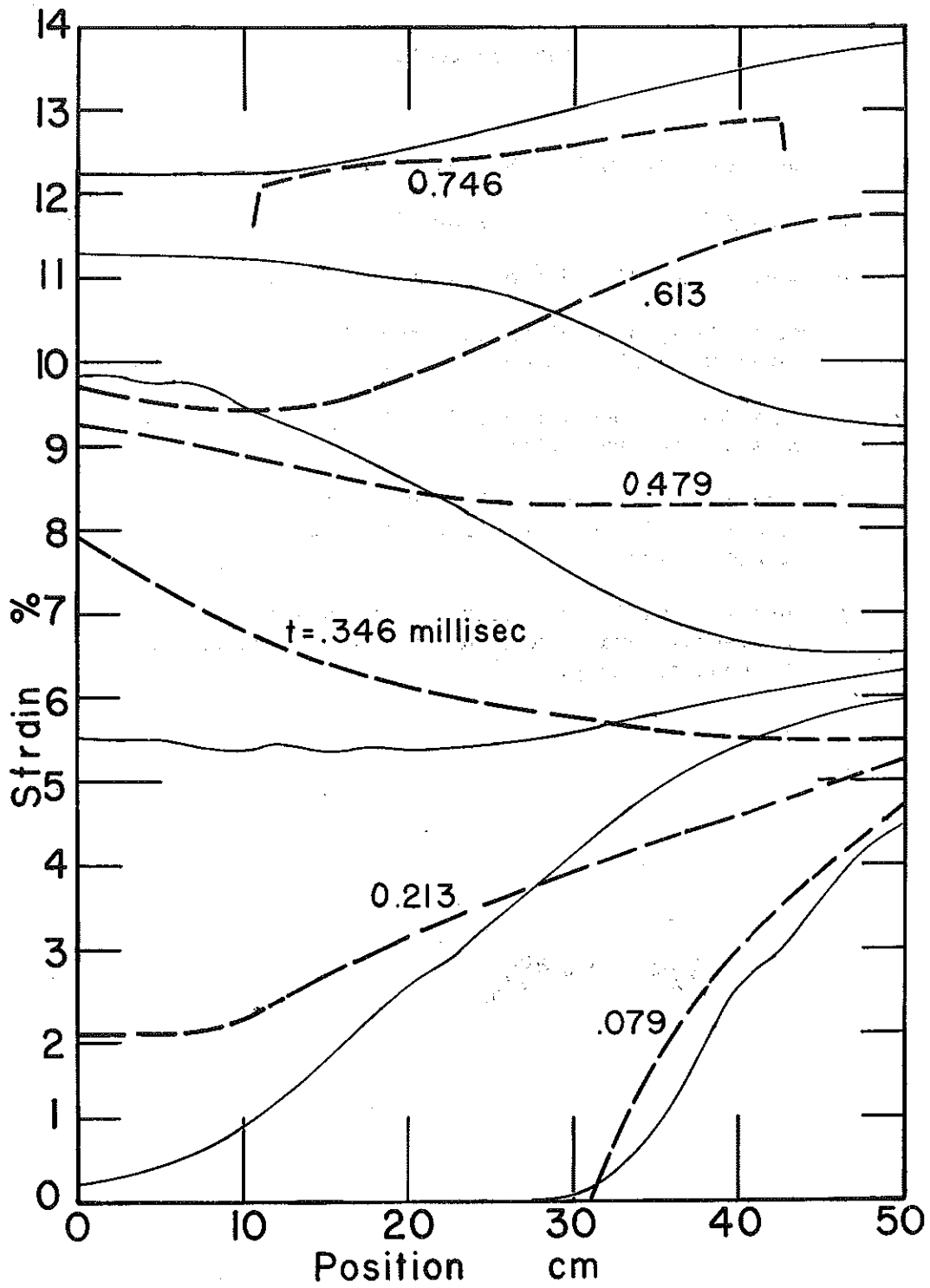
Fig. 7. Comparison of results of Run 14 (Curve C,
$\lambda = 1, \mathcal{M} = 60$), solid line; with experimental
results, broken line.

calculations shown in Fig. 2. However, the slopes of
the calculated lines in Fig. 7 do not agree with the data
and at t = 0.613 the slopes even have the wrong sign.
These facts made it seem likely that the propagation
velocities of various strain increments were incorrect.
Hence we concluded that the faults of Run 14 could not
be corrected if we continued to use curve C as our
stress-strain curve. It seemed likely that curve C had
no fundamental significance, that it was not a true curve
of a time-independent material but was the result of
trying to represent time-dependent data with a time-
independent model. Presumably, the representation was
fairly good because the experimental data came from
a single experiment with a single time scale. If a
much more rapid or much slower experiment were to be
performed, the representation based on curve C would
probably be worse.

Assuming that curve C was not of primary significance
and probably described the behavior of the material only
for one particular speed of impact, we decided to try
other stress-strain curves. The next one tried was a
simple linear curve. The result (Run 15) was judged to
be better than any previous run. In Run 16, the results
of which are shown in Fig. 8, a new stress-strain curve
was used. This curve (curve D of Fig. 6) was developed
by the same methods used to develop curve C; these
methods are described in reference 4 . Run 16 was
judged to represent the experimental data somewhat
better than Run 15 and hence was the best run made up
to that date.

After 3 unsuccessful runs (17, 18, 19), a set of
10 runs (20-29) were computed, all with linear stress-
strain curves. Various values of λ and μ were used,
and in addition the value of $R \ (= c^2/c_0^2)$ was assigned values
ranging from 1.15 down to 0.70. For a linear curve, c
is constant, of course, and assigning a value of $R \neq 1$
is simply a convenient way of changing the value of c
for the material. Of the group of 10 runs, Run 21, shown
in Fig. 9, was judged to represent the experimental data
best, and to give a slightly better fit than any of the
earlier runs.

To be useful, our model of a time-dependent material
should contain only a few disposable parameters, and
these parameters should be uniquely determined by the
experimental data. If this is the case we can use the
model with some confidence to predict the response of
the material under other experimental conditions, for
example when the impact is more rapid or slower than the
impacts we studied. The results presented in Figs. 8 and
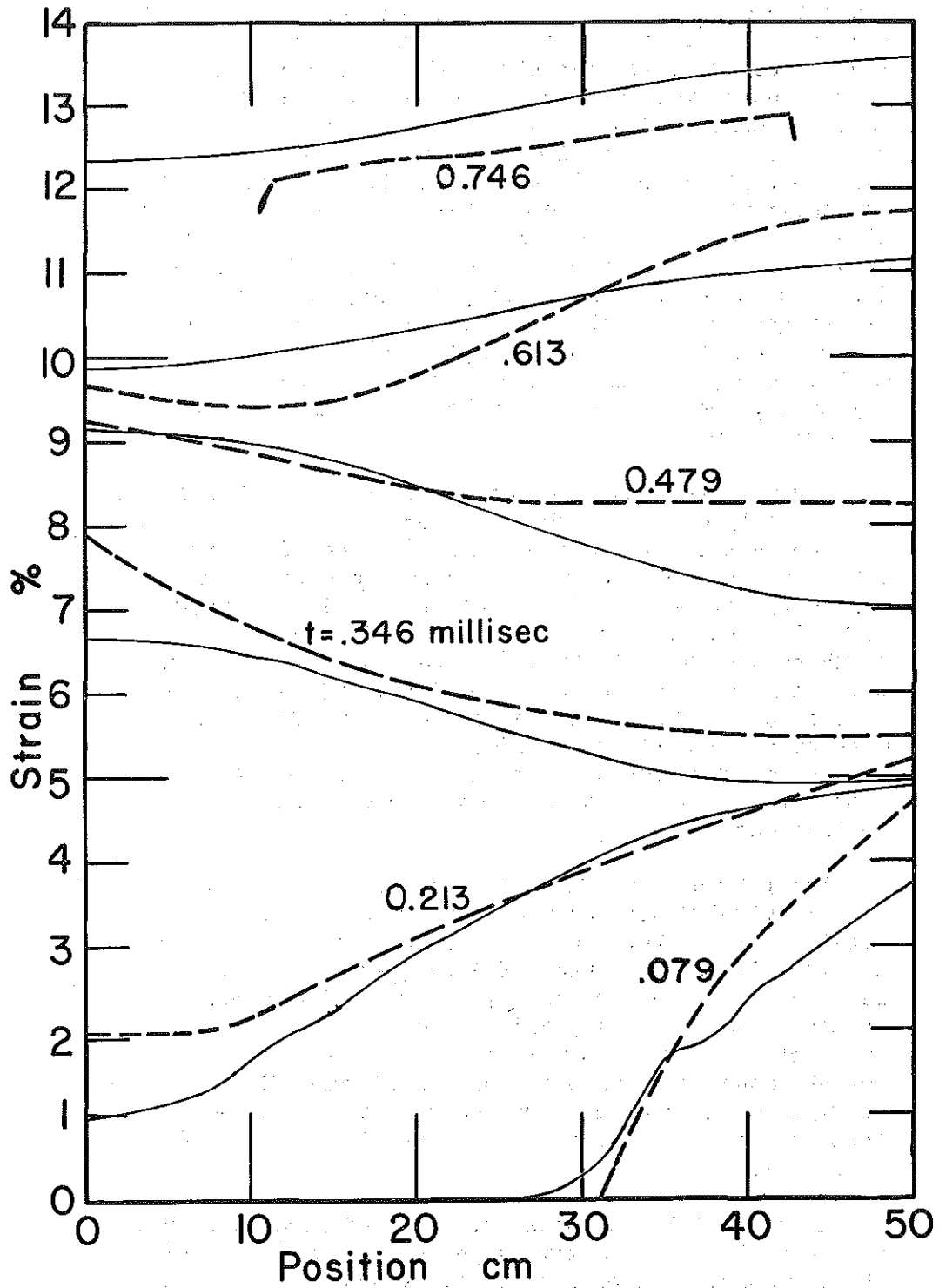9 show that our model is not unique; we were able to

Fig. 8. Comparison of results of Run 16 (Curve D,
$\lambda = 1, \mu = 60$), solid line; with experimental
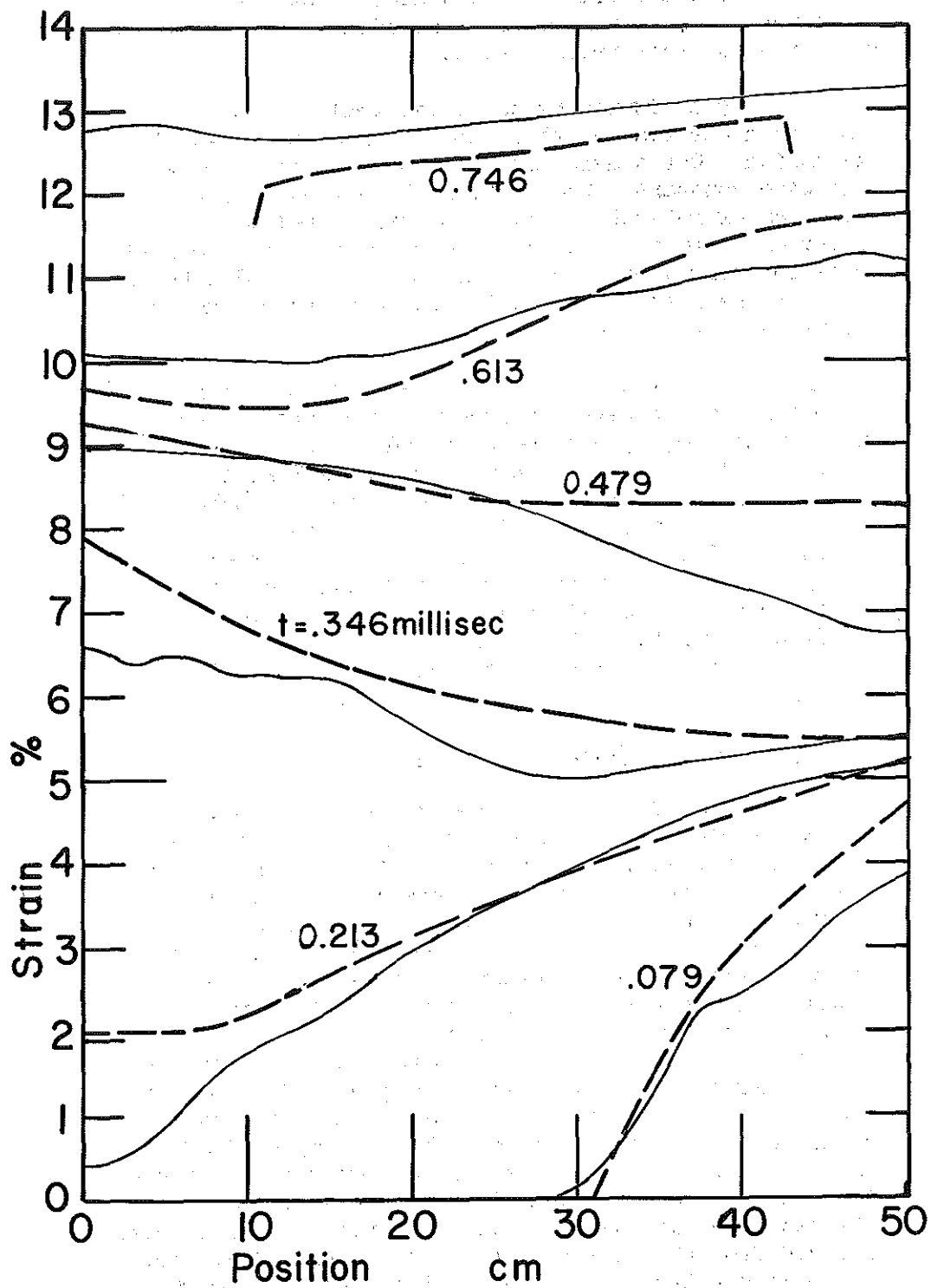results, broken line.

40

Fig. 9. Comparison of results of Run 21 (Linear
curve, R = 1.15, λ = 1, μ = 24), solid line; with
experimental results, broken line.

represent the experimental data almost equally well with different sets of parameters, including both linear and nonlinear stress-strain curves.

One way of improving our model would be to include more than one time constant in the creep and relaxation mechanism. Our single dashpot has essentially only one time constant. Some authors have used a wide spectrum of relaxation times to explain polymeric behavior. However, we would need to have experimental data covering a wider range of impact velocities before we would be justified in introducing a larger number of elements into our model.

Since observations of impact at substantially higher velocities would have required major changes in our experimental equipment, we searched for other ways to cast more light on the behavior of our material. The set of experimental data analyzed above were taken with a specimen 50 cm long. This length was short enough so that reflections of the strain pulse occurred during the period of observation. The reflection of strains into the already-strained material made the data more difficult to interpret. We decided to perform experiments in which reflections did not occur. Two such experiments are described in the following section.

6.   Experiments Without Reflections

Specimens of nylon yarn 400 cm long (8 times the normal length) were marked in the usual way at 1-cm intervals and installed in the usual way. The camera was aimed at the end of the specimen where impact occurred, so that it could photograph a length of roughly 50 cm of the yarn. The yarn was so long that the photographing was completed before the strain pulse could be reflected at the fixed end of the string and be propagated back into the field of the camera. After a considerable amount of work (synchronization of the impact and the photographing was a problem), two good photos of impact behavior were obtained. The data obtained from these photos have been designated NC-6 and NC-7. Fig. 10 shows the photo from which NC-6 was obtained. Figures 11 and 12 show typical curves plotted from each set of data. The plotted points were derived from the data and the curves were faired thru the points (they are not computed curves). In each figure the top curve refers to the end of the yarn attached to the head mass and the bottom curve refers to a point near the other edge of the field of view of the camera; the middle curve refers to a point intermediate between the other two. The two figures show strain as a function of time for periods of about
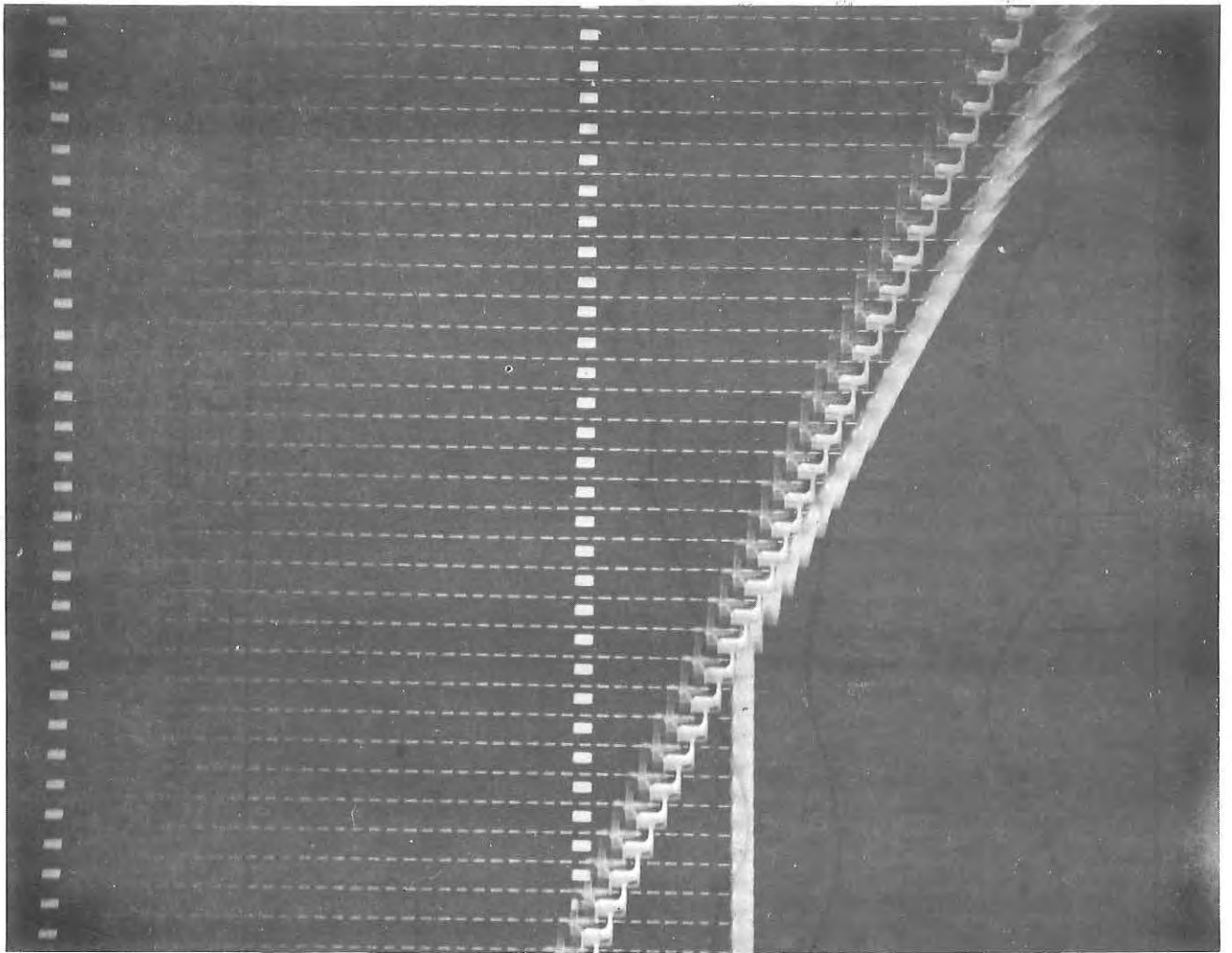
Fig. 10. Photograph from which the data designated NC-6 were obtained.
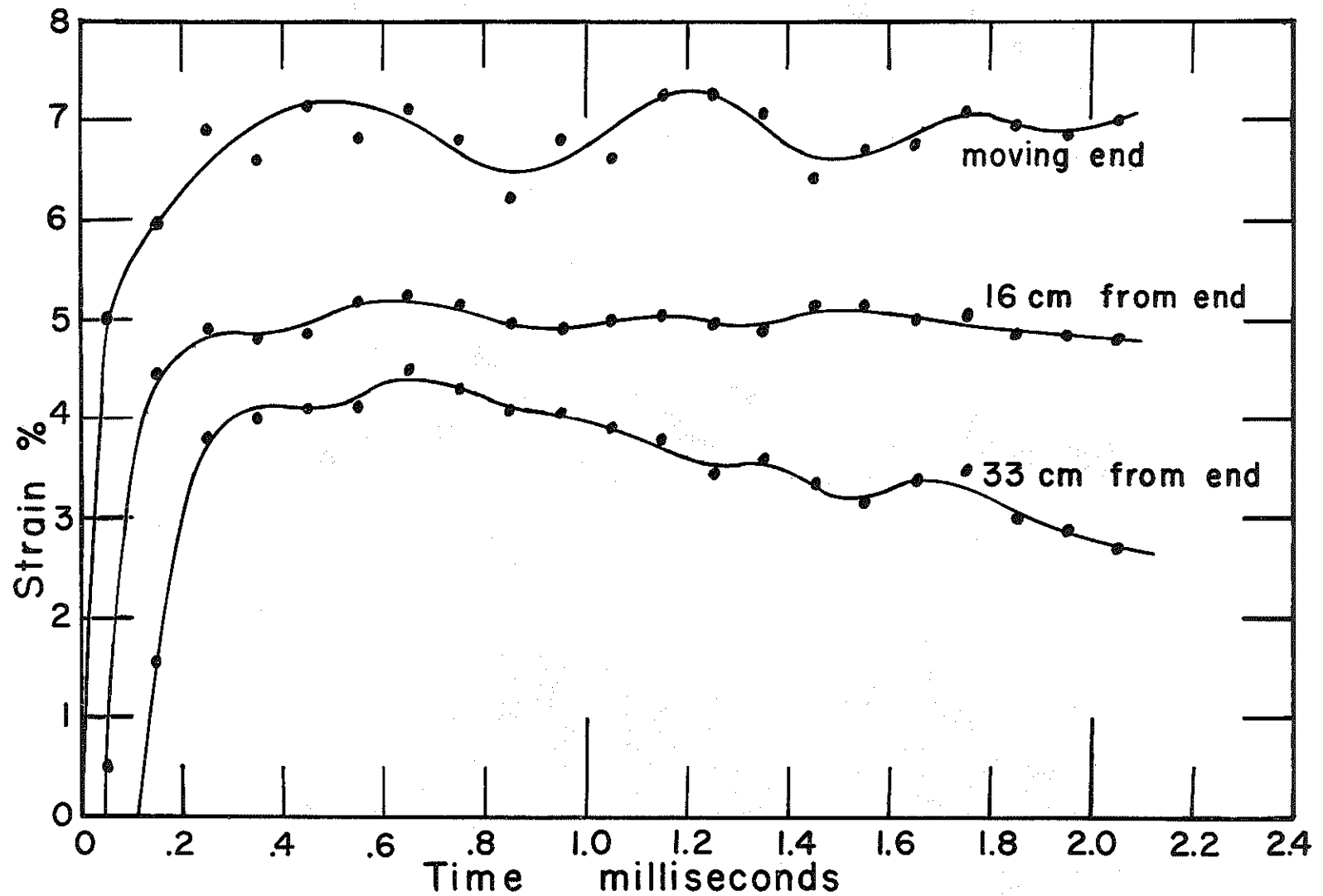
Fig. 11. Selected data from the experiment NC-6. Strain versus time after impact. Each curve refers to a different point on the specimen.
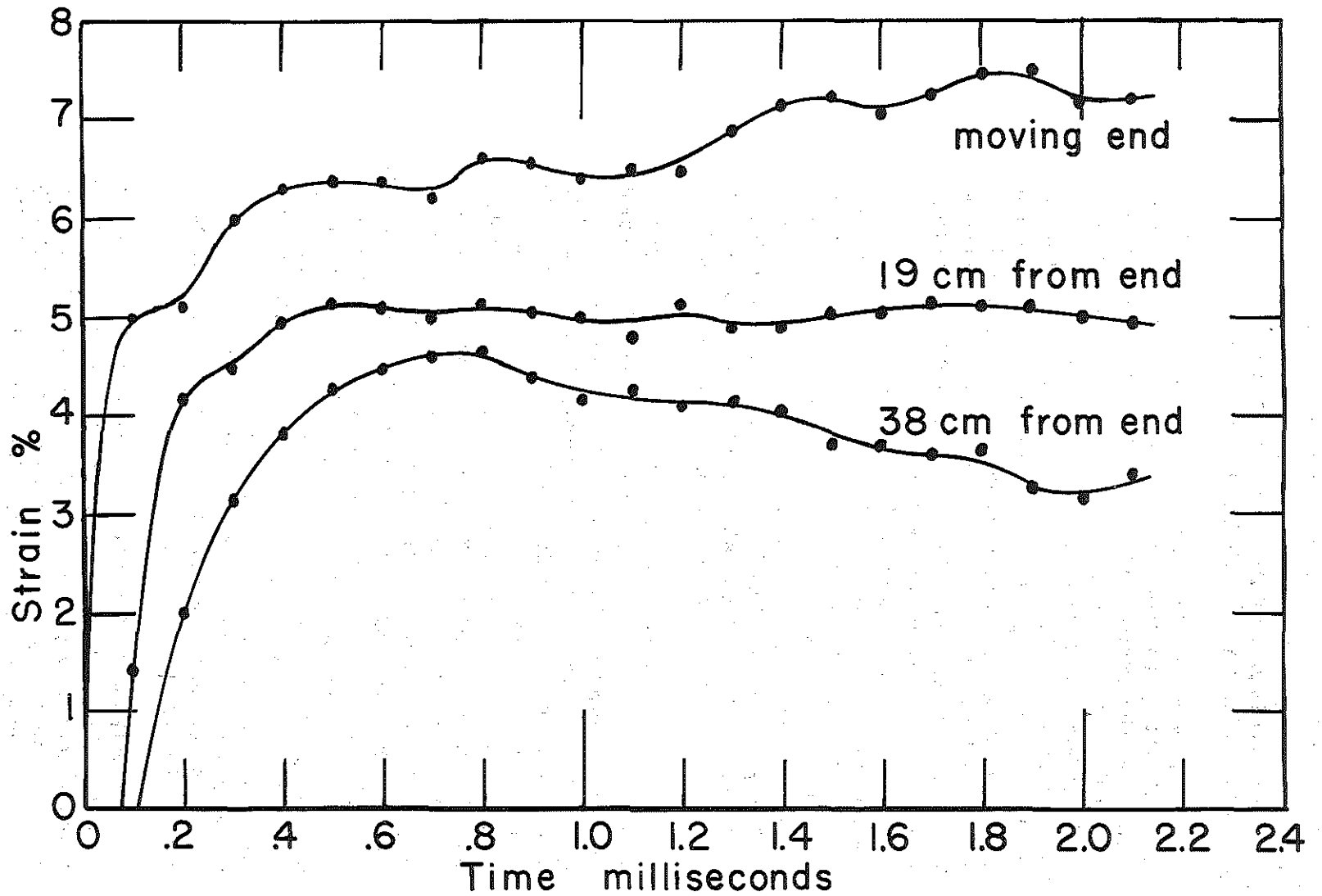
44

Fig. 12. Selected data from the experiment NC-7. Strain versus time after impact. Each curve refers to a different point on the specimen.

2 milliseconds after impact. For details of how the high-speed, stroboscopic photographs were taken and how the data (positions of marks on the strings) were analyzed, reference 4 should be consulted.

We had expected all curves of the type shown in Figs. 11 and 12 to show an initial rapid rise corresponding to the arrival of the strain pulse, followed by a gradual rise corresponding to a further stretching of the material. Of the six curves plotted, only the top curve in Fig. 12 shows this behavior. The top curve in Fig. 11 and the middle curve in Fig. 12 show essentially no change in strain after the passage of the initial pulse. The three remaining curves all show a decrease of strain with time. Instead of continuing to elongate by creep, the material represented by these curves appears to be contracting after it reaches maximum strain. There are wide variations in strain at different points on the specimen at a given time and also at a given point at different times. For example, Fig 11 at t=2 msec has a strain of about 7% near the head mass and a strain of less than 3% at the point 33 cm downstring. Also, at the 33 cm point the strain went above 4% at 0.6 msec and then fell to below 3%.

The strains shown in Figs. 11 and 12 show major departures from the behavior that is commonly assumed, in which a strain pulse of constant height travels along the specimen, leaving uniformly strained material behind it. The possibility that the data are in error because of experimental difficulties has been considered, but we are not aware of anything that could invalidate these two experiments. The fact that one of the curves in Figs. 11 and 12 slants upward, two are horizontal and three slant downward does not point toward any simple type of experimental error. Wavelike irregularities are evident in some of the curves, especially in the two top curves that describe the point nearest the head mass. Such waves have been observed in many of our experiments and have amplitudes that sometimes exceed twice the scatter of the data. We believe that the waves actually exist but can only speculate on their cause. One possible cause is non-uniformity of the nylon yarn.

The mathematically simple picture of impact is one in which the head mass is instantly accelerated to some fixed velocity and travels with constant speed thereafter. Our actual experiments differed significantly from this simple picture. The head mass had a finite velocity-rise time of roughly 0.3 msec, as can be seen from Figs. 11 and 12 (the head mass velocity is very nearly the same as the particle velocity at x=o).

After the head mass reaches its maximum speed it
gradually slows down because of friction and because
of the force exerted on it by the stretching specimen,
but the deceleration is too small to be very noticeable
in Figs. 11 and 12. The acceleration and deceleration
of the head mass complicate the situation somewhat
but do not give any obvious help in explaining the
curves shown in Figs. 11 and 12.

7. Attempts to Calculate the No-Reflection Data

The data taken in such a way as to avoid strain-
pulse reflections in the part of the specimen being
observed were analyzed by the same methods as were used
in section 5. It was realized that if our model of
the material was a good one it should predict the be-
havior when reflections were present and also when they
were not present. Thirteen computer runs (30 - 42)
were made, using a variety of combinations of the
constants λ, μ and R and various types of stress-
strain curves, including linear "curves" and curve C
of Fig. 6. Since the specimen length was now 8 times
what it had previously been, the distance between
points of the computation lattice was increased from
1 cm to 2 cm. Even so the computer time per run was
considerably increased, because all lattice points in
each row had to be computed, although the strain at
most of them had not begun to rise above zero.

None of the 13 runs gave curves that looked like
those in Figs. 11 and 12. A few of the calculated
curves are shown in Fig. 13. In only one run did we
succeed in getting the strain to decrease with time;
this was Run 32. The three curves for different values
of x differ from the experimental curves, however, in
that all three calculated curves approach each other
and become nearly coincident. The experimental curves
never get very close together and are diverging as the
experiment ends.

It seems best not to try to propose any specific
mechanism for the behavior shown in Figs. 11 and 12.
The results were unexpected and interesting; they
cast some doubt on the validity of our three-element
model. However, it should be remembered that large
amounts of energy are released when the slider is
accelerated by the rubber bands. Energy could travel
more rapidly in the steel tracks and possibly in
the supporting table than it travels in the nylon
yarn. It seems doubtful that any mechanism exists
that could transfer energy to the fixed end of the
string and set it in motion before the pulse in the
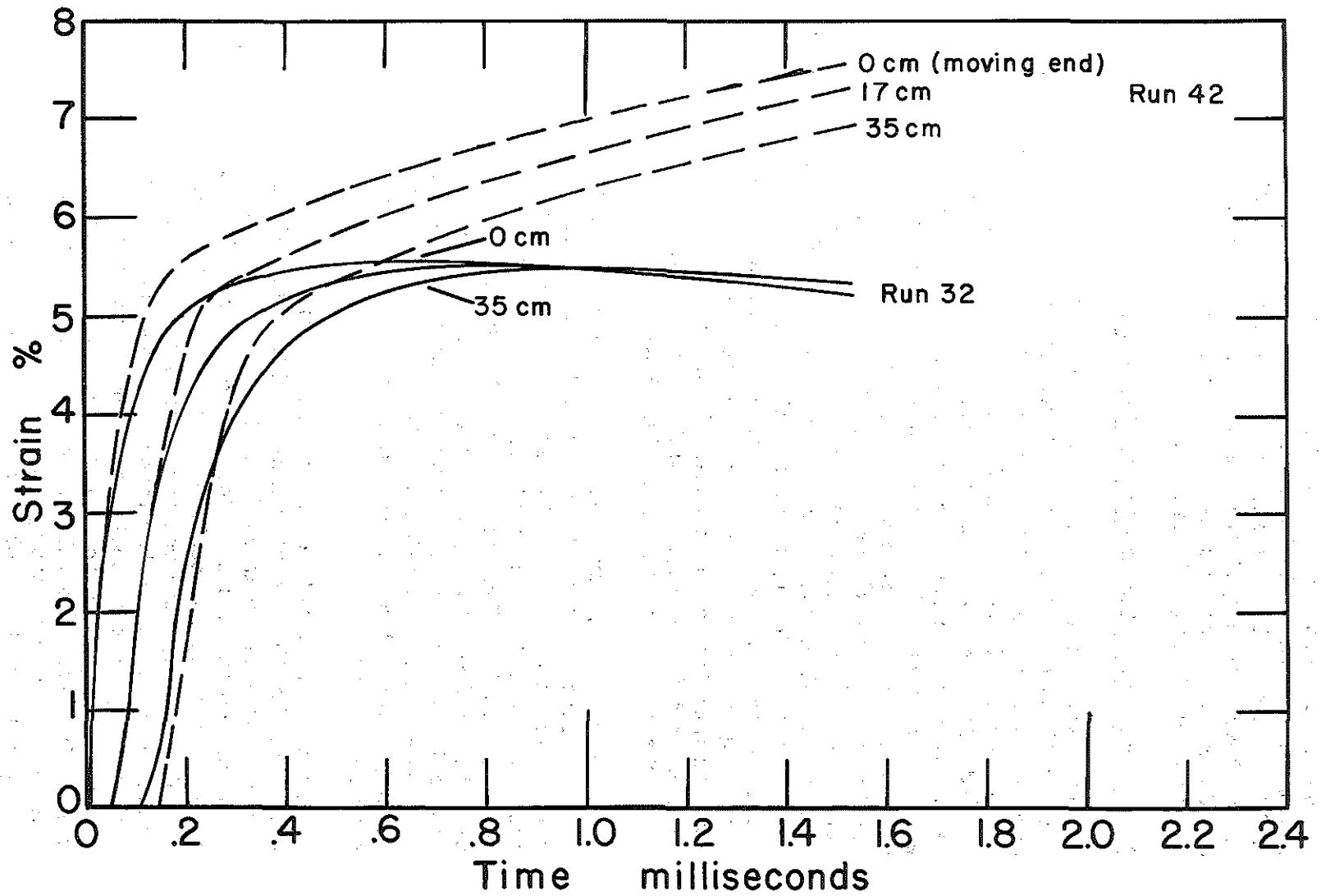string arrived, but some such mechanism cannot be

47

Fig. 13. A few of the curves calculated in our attempts to match the curves in Figs. 11 and 12.

completely ruled out. Further experiments are needed,
in which the conditions and parameters of the experiment
are varied.

8. Conclusions

The integral-equation, successive-substitution
method of analyzing and predicting the behavior of
materials under tensile impact has been extended to
include time-dependency (creep and relaxation). A
three-element model, consisting of a spring and dashpot
in parallel, and a second spring in series with this
combination was used. The behavior of short (50 cm)
specimens, in which the strain pulse experienced re-
flections, could be explained by this model. It was
in fact possible to describe the behavior with various
models, employing different stress-strain curves
and other different model parameters. Since different
sets of parameters described the observed behavior
almost equally well, no unique set of parameters for
the material could be chosen.

When long specimens were used, in which no re-
flections could occur during the time of the ex-
periment, no satisfactory model of the process was
found. The material was observed to contract after
the strain pulse had passed over it instead of re-
maining at constant strain or continuing to elongate
slightly. A study of this somewhat-unexpected be-
havior appears to be the most fertile area for future
work, when and if impact experiments are resumed.

A-1 Determination of λ and μ

The purpose of this appendix is to record certain ideas that were being considered when work on this project was discontinued. These have to do with determining λ and μ more precisely. At present we have too much freedom in their choice; hence we shall consider additional restrictions which can be applied experimentally. We note that the use of the parameter λ implies that the two springs are of the same nature, and differ only in length, spring 2 being λ times as long as spring 1.

Determination of λ. Noting Fig. 3 and equations (10) - (14), we see that under slow (quasistationary) loading $\sigma_1 = 0$, and

$$\frac{d\sigma}{d\epsilon} = \sigma'(\epsilon_1)\frac{d\epsilon_1}{d\epsilon} = \frac{\sigma'(\epsilon_1)}{1+\lambda}. \tag{1a}$$

Under fast loading

$$\dot{\sigma} = \sigma'(\epsilon_1)\,\dot{\epsilon}_1 = \sigma'(\epsilon_1)\left[\dot{\epsilon} - \dot{\epsilon}_2\right]. \tag{2a}$$

Initially $\sigma_1 = 0$; hence $\dot{\epsilon}_2 = 0$, and (2a) becomes

$$\dot{\sigma} = \sigma'(0)\,\dot{\epsilon} \quad \text{when } t = 0. \tag{3a}$$

It follows that

$$\frac{d\sigma}{d\epsilon} = \sigma'(0) \quad \text{when } t = 0. \tag{4a}$$

51

Placing the initial value $\epsilon_1 = 0$ in (1a) and dividing into (4a), we obtain finally

$$\lambda = \frac{\left(\dfrac{d\sigma}{d\epsilon}\right)_{OF}}{\left(\dfrac{d\sigma}{d\epsilon}\right)_{OS}} - 1 \tag{5a}$$

where the subscripts O, F, and S indicate "initial", "fast", and "slow", respectively. This gives λ after the derivatives on the right hand side have been determined experimentally.

Determination of μ. Let us suppose that the springs are linear, and have spring constants K_1 and K_2, respectively. We then have

$$\left. \begin{array}{c} \dot{\epsilon} = \dot{\epsilon}_1 + \dot{\epsilon}_2 , \\[2mm] \sigma = K_1 \epsilon_1 = \sigma_1 + \sigma_2 = K_2 \epsilon_2 + \mu \dot{\epsilon}_2 . \end{array} \right\} \tag{6a}$$

Starting at t=o with the system unstressed let us maintain $\dot{\epsilon} = 1$, then

$$\left. \begin{array}{c} \dot{\epsilon}_1 + \dot{\epsilon}_2 = 1 \\[2mm] K_1 \epsilon_1 - K_2 \epsilon_2 - \mu \dot{\epsilon}_2 = 0 . \end{array} \right\} \tag{7a}$$

Taking Laplace transforms we have

$$\left. \begin{array}{c} s \bar{\epsilon}_1 + s \bar{\epsilon}_2 = \dfrac{1}{s} \\[2mm] K_1 \bar{\epsilon}_1 - (K_2 + \mu s) \bar{\epsilon}_2 = 0 \end{array} \right\} \tag{8a}$$

52

where the bars indicate transforms. Solving for $\bar{\epsilon}_1$, we obtain

$$\bar{\epsilon}_1 = \frac{-\frac{1}{\Delta}(K_2 + \mu\Delta)}{-\Delta(K_2 + \mu\Delta + K_1)}$$

$$= \frac{K_2}{\mu\Delta^2(\Delta+\alpha)} + \frac{1}{\Delta(\Delta+\alpha)} \Bigg\} \quad (9a)$$

where

$$\alpha = \frac{K_1 + K_2}{\mu}. \qquad (10a)$$

Noting the partial fraction expansions

$$\frac{1}{\Delta^2(\Delta+\alpha)} = \frac{1}{\alpha\Delta^2} - \frac{1}{\alpha^2\Delta} + \frac{1}{\alpha^2(\Delta+\alpha)}$$

$$\frac{1}{\Delta(\Delta+\alpha)} = \frac{1}{\alpha\Delta} - \frac{1}{\alpha(\Delta+\alpha)}, \Bigg\} \quad (11a)$$

and using a table of Laplace transforms we find that the inverse transform of (9a) is

$$\epsilon_1 = \frac{K_2}{\mu\alpha}t + \frac{1}{\alpha}\left(1 - \frac{K_2}{\mu\alpha}\right)\left(1 - e^{-\alpha t}\right). \quad (12a)$$

Multiplying by K_1 to obtain σ, and noting (10a) we obtain finally

$$\sigma = \frac{K_1 K_2}{K_1 + K_2}t + \mu\left(\frac{K_1}{K_1+K_2}\right)^2\left(1 - e^{-\alpha t}\right). \quad (13a)$$

Differentiating with respect to t gives

$$\dot{\sigma} = \frac{K_1 K_2}{K_1 + K_2} + \frac{K_1^2}{K_1 + K_2} e^{-\alpha t}, \quad (14a)$$

from which we see that $\dot{\sigma}$ changes exponentially from one value to another with a time constant

$$\tau = \frac{1}{\alpha} = \frac{\mu}{K_1 + K_2} \ .$$

(15a)

We also note that the first term in (14a) is the spring constant of springs 1 and 2 in series. If τ is determined experimentally, (15a) gives μ .

A-2 Further Constraints. Inclusion of Inertia.

In the above it was tentatively assumed that the experiments devised were such that inertia is unimportant. If this is not the case we can still proceed as follows if the springs are linear. We have the equations

$$
\left.
\begin{array}{cc}
\rho \dfrac{\partial^2 \omega}{\partial t^2} = \dfrac{\partial \sigma}{\partial x}, & \sigma = \sigma_1 + \sigma_2, \\[2mm]
\sigma_1 = \mu \dfrac{\partial \epsilon_2}{\partial t}, & \epsilon = \epsilon_1 + \epsilon_2, \\[2mm]
\sigma = K_1 \epsilon_1, & \sigma_2 = K_2 \epsilon_2.
\end{array}
\right\} \tag{16a}
$$

It follows that

$$
\rho \frac{\partial^2 \omega}{\partial t^2} = K_1 \frac{\partial \epsilon_1}{\partial x}, \tag{17a}
$$

$$
K_1 \epsilon_1 - K_2 \epsilon_2 = \sigma - \sigma_2 = \sigma_1 = \mu \frac{\partial \epsilon_2}{\partial t}. \tag{18a}
$$

In view of (16a) this may be written

$$
(K_1 + K_2)\epsilon_1 - K_2 \epsilon = \mu \left(\frac{\partial \epsilon}{\partial t} - \frac{\partial \epsilon_1}{\partial t} \right). \tag{19a}
$$

Differentiating with respect to x gives

$$
\left.
\begin{array}{l}
(K_1 + K_2)\dfrac{\partial \epsilon_1}{\partial x} - K_2 \dfrac{\partial \epsilon}{\partial x} \\[3mm]
\qquad = \mu \left(\dfrac{\partial^2 \epsilon}{\partial x \partial t} - \dfrac{\partial^2 \epsilon_1}{\partial x \partial t} \right).
\end{array}
\right\} \tag{20a}
$$

55

Substituting from (17a) this becomes

$$(K_1 + K_2) \frac{\rho}{K_1} \frac{\partial^2 s}{\partial t^2} - K_2 \frac{\partial \epsilon}{\partial x} \\ = \mu \left(\frac{\partial^2 \epsilon}{\partial x \partial t} - \frac{\rho}{K_1} \frac{\partial^3 s}{\partial t^3} \right), \qquad (21a)$$

Since

$$\lambda = \frac{K_1}{K_2} \qquad (22a)$$

(21a) may be written

$$\left(1 + \frac{1}{\lambda} \right) \frac{\partial^2 s}{\partial t^2} - \frac{K_1}{\rho} \frac{1}{\lambda} \frac{\partial \epsilon}{\partial x} \\ = \frac{\mu}{\rho} \left(\frac{\partial^2 \epsilon}{\partial x \partial t} - \frac{\rho}{K_1} \frac{\partial^3 s}{\partial t^3} \right), \qquad (23a)$$

or

$$\frac{1}{\lambda} \left(\frac{\partial^2 s}{\partial t^2} - c^2 \frac{\partial \epsilon}{\partial x} \right) \\ - \frac{\mu}{\rho} \frac{\partial}{\partial t} \left(\frac{\partial \epsilon}{\partial x} - \frac{1}{c^2} \frac{\partial^2 s}{\partial t^2} \right) = - \frac{\partial^2 s}{\partial t^2}, \qquad (24a)$$

where

$$c^2 = \frac{K_1}{\rho} . \qquad (25a)$$

Placing

$$f(x,t) = \frac{\partial^2 s}{\partial t^2} - c^2 \frac{\partial \epsilon}{\partial x} \\ = \frac{\partial^2 s}{\partial t^2} - c^2 \frac{\partial^2 s}{\partial x^2} \qquad (26a)$$

(24a) becomes

$$\frac{\mu}{\rho c^2} \frac{\partial f}{\partial \tau} + \frac{1}{\lambda} f = -\frac{\partial^2 \Delta}{\partial t^2}. \qquad (27a)$$

$\frac{\partial^2 \Delta}{\partial x^2} = \frac{\partial f}{\partial x}$ and $\frac{\partial^2 \Delta}{\partial t^2}$ are obtained from test data. For an assumed value of c - perhaps the initial "wave velocity"— $\mu/\rho c^2$ and $1/\lambda$ can be determined using least squares in connection with (27a), which is written for several points in the xt plane. We note that (27a) is linear in $1/\lambda$ and $\mu/\rho c^2$.

An approximation to c^2 can also be obtained from (25a), in which we place

$$K_1 = (1 + \lambda) K, \qquad (28a)$$

wherein K is the spring constant of both springs in series - obtained by a slow (quasistationary) test - and λ is a tentative value which is later improved.

57

A-3 Further Constraints. Use of Sinusoidal Excitation.

In addition to tests involving transient motion it is
also possible to devise tests involving sinusoidal
motion, or vibration. For example, let us consider
a string of length L fastened at the origin and ex-
tending to point L on the x axis, Fig. 14. At the
right end x=L it is fastened to a device capable of
exerting tension, both constant and sinusoidal of
angular frequency ω . First we prestretch the string
so that it has a constant strain ϵ_0 ; and then super-
impose a small sinusoidal motion on this. In the
treatment which follows $K_1 = \sigma'(\epsilon_{10})$ where ϵ_{10} is
the initial value of ϵ_1, $K_2 = K/\lambda$ and σ, σ_1, σ_2, ϵ,
ϵ_1, ϵ_2, Δ, Δ_1, and Δ_2 are the sinusoidal parts of
the stresses, strains, and displacements which are
the excess over the prestressed values. (Incremental
stresses, strains, and displacements.)

Using complex notation to take care of the
sinusoidally varying quantities, as is commonly done
in solving alternating current network and transmission
line problems, beam vibration problems, etc., our basic
equations become

$$-\rho \omega^2 \bar{\Delta} = \frac{d\bar{\sigma}}{dx} , \qquad (29a)$$

$$\bar{\sigma} = \bar{\sigma}_1 + \bar{\sigma}_2 , \qquad (30a)$$

$$\bar{\epsilon} = \bar{\epsilon}_1 + \bar{\epsilon}_2 , \qquad (31a)$$

$$\bar{\sigma} = K_1 \bar{\epsilon}_1 , \qquad (32a)$$

$$\bar{\sigma}_1 = \mu j \omega \bar{\epsilon}_2 , \qquad (33a)$$

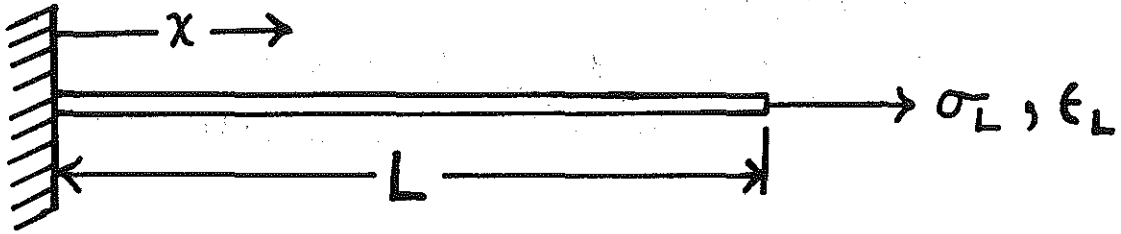$$\bar{\sigma}_2 = K_2 \bar{\epsilon}_2 , \qquad (34a)$$

58

Fig. 14. String subjected to special end conditions.

where the bars indicate the complex quantities which
correspond to the various sinusoidally varying
quantities, and j is the imaginary unit. It follows
that

$$\bar{\sigma} = \bar{\sigma_1} + \bar{\sigma_2}$$

$$= (K_2 + j\omega\mu)\bar{\epsilon_2} = K_1\bar{\epsilon_1}, \qquad (35a)$$

$$\bar{\epsilon} = \bar{\epsilon_1} + \bar{\epsilon_2}$$

$$= \bar{\epsilon_1}\left[1 + \frac{K_1}{K_2 + j\omega\mu}\right] = \frac{\bar{\sigma}}{K_1}\left(\frac{K_1 + K_2 + j\omega\mu}{K_2 + j\omega\mu}\right). \qquad (36a)$$

Placing

$$\frac{\rho\omega^2(K_1 + K_2 + j\omega\mu)}{K_1(K_2 + j\omega\mu)} = \alpha^2, \qquad (37a)$$

(29a) and (36a) give

$$\frac{d\bar{\epsilon}}{dx} + \alpha^2\bar{\lambda} = 0, \qquad (38a)$$

or

$$\frac{d^2\bar{\lambda}}{dx^2} + \alpha^2\bar{\lambda} = 0. \qquad (39a)$$

The general solution of this differential
equation is

$$\bar{\lambda} = A\sin\alpha x + B\cos\alpha x \qquad (40a)$$

where A and B are constants. Applying the boundary conditions

$$\bar{\lambda} = 0 \quad when \quad x = 0, $$
$$\bar{\lambda} = \bar{\lambda}_L \quad when \quad x = L, \left.\right\} \quad (41a)$$

we obtain

$$0 = B$$
$$\bar{\lambda}_L = A \sin \alpha L \,; \left.\right\} \quad (42a)$$

which in (40a) give finally

$$\bar{\lambda} = \bar{\lambda}_L \frac{\sin \alpha x}{\sin \alpha L} \, . \quad (43a)$$

Differentiating with respect to x we obtain also

$$\bar{E} = \bar{\lambda}_L \alpha \frac{\cos \alpha x}{\sin \alpha L} \, . \quad (44a)$$

In view of (32a) - (36a) it follows that

$$\bar{E}_1 = \bar{E} \left(\frac{K_2 + j \omega \mu}{K_1 + K_2 + j \omega \mu} \right), \quad (45a)$$

$$\bar{E}_2 = \bar{E}_1 \left(\frac{K_1}{K_2 + j \omega \mu} \right) = \bar{E} \left(\frac{K_1}{K_1 + K_2 + j \omega \mu} \right), \quad (46a)$$

$$\bar{\sigma}_1 = j \omega \mu \bar{E}_2, \quad (47a)$$

61

$$\bar{\sigma}_2 = K_2 \bar{\epsilon}_2 , \qquad (48a)$$

$$\bar{\sigma} = K_1 \bar{\epsilon}_1 = \bar{\epsilon} \left[\frac{K_1 (K_2 + j\omega\mu)}{K_1 + K_2 + j\omega\mu} \right] . \qquad (49a)$$

Substituting (44a) in (49a) we obtain

$$\bar{\sigma} = \bar{\Delta}_L \, \alpha \left[\frac{K_1 (K_2 + j\omega\mu)}{K_1 + K_2 + j\omega\mu} \right] \frac{\cos \alpha x}{\sin \alpha L} . \qquad (50a)$$

or, noting (37a),

$$\bar{\sigma} = \bar{\Delta}_L \left(\frac{\rho\omega^2}{\alpha} \right) \frac{\cos \alpha x}{\sin \alpha L} . \qquad (51a)$$

At the end x=L this becomes

$$\bar{\sigma}_L = \bar{\Delta}_L \left(\frac{\rho\omega^2}{\alpha} \right) \cot \alpha L , \qquad (52a)$$

which may be written

$$\beta \tan \beta = \rho\omega^2 L \left(\frac{\bar{\Delta}_L}{\bar{\sigma}_L} \right) , \qquad (53a)$$

where

$$\beta = \alpha L . \qquad (54a)$$

For any value of ω we can obtain $\bar{A}_L/\bar{\sigma}_L$ experimentally. (53a) then gives β, after which (54a) gives α. *We thus know α as a function of ω. This knowledge is used in connection with (37a) in order to obtain K_1, K_2, and μ.

In so doing it may be desirable to take advantage of the fact that the spring contant K for both springs in series is

$$K = \frac{K_1 K_2}{K_1 + K_2},$$
(55a)

which relation can be used to reduce the number of unknowns by one if we are willing to determine K separately by obtaining a <u>slow test</u> value of $d\sigma/d\epsilon$ evaluated at $\epsilon = \epsilon_0$.

In any case we can write (37a) in the form

$$\rho\omega^2(K_1 + K_2 + j\omega\mu)$$
$$- K_1(K_2 + j\omega\mu)\alpha^2 = 0,$$
(56a)

insert the successive pairs of values (ω_1, α_1), (ω_2, α_2), ... (ω_m, α_m) obtained by experiment, (53a), and (54a); and determine the unknowns so that

$$\sum_{i=1}^{m} \left| \rho\omega_i^2(K_1 + K_2 + j\omega_i\mu) \right.$$
$$\left. - K_1(K_2 + j\omega_i\mu)\alpha_i^2 \right|^2 = minimum.$$
(57a)

---

* β can be determined from (53a) in several different manners, among which are the following.

1. An interation procedure can probably be devised.

2. An interpolation procedure can certainly be devised.

3. Using a digital computer a table of values of the function $\beta \tan \beta$ for complex arguments can easily be constructed.

In so doing a digital computer can be used to cover the ranges of the unknowns - two or three as the case may be, and choose the best combination of values.

Even without a digital computer it is likely that a least square procedure can be devised.

Another possibility is to write (37a) in the form

$$\rho \omega^2 \left(1 + j\omega \frac{\mu}{K_1 + K_2} \right)$$

$$= \alpha^2 \left(\frac{K_1 K_2}{K_1 + K_2} + j\omega \frac{K_1 \mu}{K_1 + K_2} \right), \qquad (58a)$$

or

$$\rho \omega^2 X_1 - \alpha^2 X_2$$

$$- j\rho\omega + j\frac{\alpha^2 K}{\omega} = 0 \qquad (59a)$$

where

$$X_1 = \frac{\mu}{K_1 + K_2} , \quad X_2 = \frac{K_1 \mu}{K_1 + K_2} . \qquad (60a)$$

K is obtained separately, as indicated in connection with (55a); then since X_1 and X_2 appear linearly in (59a), a least square procedure can easily be devised to determine them so that

$$\sum_{i=1}^{n} \left| \rho \omega_i^2 X_1 - \alpha_i^2 X_2 - j\rho \omega_i + j\frac{\alpha_i^2 K}{\omega_i} \right|^2 = \text{minimum}. \qquad (61a)$$

Knowing X_1, X_2, and K, the other quantities K_1, K_2, and μ follow immediately.

Since K appears linearly in (59a) it could, if desired, be included among the unknowns instead of being determined by a separate experiment.

64